Development of Magneto-organogel and study of gold nanoparticles growth

A dissertation submitted
in partial fulfilment

FOR THE DEGREE
OF
MASTER OF SCIENCE IN CHEMISTRY

Under The Academic Autonomy
NATIONAL INSTITUTE OF TECHNOLOGY, ROURKELA

By

Abhinav Mohanty

Under the Guidance of
Prof. Supratim Giri

DEPARTMENT OF CHEMISTRY
NATIONAL INSTITUTE OF TECHNOLOGY
ROURKELA – 769008, ODISHA

TABLE OF CONTENTS

CERTIFICATE OF STUDY

National Institute of Technology
Rourkela

This is certify that **Mr. Abhinav Mohanty**, student of Integrated M.Sc. in Chemistry (2010-2015), in NIT Rourkela, Odisha, has carried out his dissertation work on "***Development of Magneto-organogel and study of gold nanoparticles growth***" under my supervision and guidance as a partial fulfillment of the degree of M.Sc. in Chemistry. The thesis embodies original work done by him and deserves merit for consideration for the degree. No results or any part of the result have been submitted anywhere for degree or equivalent qualification.

Date: **Supratim Giri**

Place: NIT Rourkela (supervisor)

ACKNOWLEDGEMENT

With deep regards and profound respect, I avail the opportunity to express my deep sense of gratitude and indebtedness to **Prof. Supratim Giri**, Department of Chemistry, National Institute of Technology, Rourkela, for introducing the present project topic and for his inspiring guidance, constructive criticism and valuable suggestions throughout the project work. I gratefully acknowledge his constant encouragement and help in different ways to complete this project successfully.

I acknowledge my sincere regards to **Prof. N. Panda (HOD, Dept. of Chemistry)** and all the faculty members, Department of Chemistry, NIT Rourkela for their enthusiasm in promoting the research in chemistry and for their kindness and dedication to students. I am extremely grateful to **Prof. Kunal Pal**, Department of Biotechnology and Medical Engineering, National Institute of Technology, Rourkela for his constant help and guidance during the course of this project work. I would like to add a special note of thanks to **Mr. Balmiki Kumar and Mrs. Souymashree Dhal**, Ph.D. Scholars, Department of Chemistry for their kind help and guidance whenever required.

I acknowledge the support of my classmates and lab mates throughout this course. Last but not the least, I also take the privilege to express my deep sense of gratitude to my parents, for selflessly extending their ceaseless help and moral support at all time.

Abhinav Mohanty

ABSTRACT

The current research project work basically deals with two areas- iron oxide nanoparticles and gold nanoparticles. Synthesis of magnetic nanoparticles was carried out using co-precipitation method and then oleylamine functionalized Fe_3O_4 nanoparticles were synthesized by thermal decomposition method. Oleylamine capping not only prevented the aggregation of nanoparticles but also made the nanoparticles soluble in organic mediums such as hexane; chloroform etc. in order to make the nanoparticles suitable for organogel formation. We have reported two types of magneto-organogels; one based on oleic acid while the other based on soybean oil and their characterization was carried out using XRD, FESEM, FTIR and microscopic analysis. The release kinetics studies and preliminary impedance analysis projects the magneto-organogels as potential agents for controlled drug delivery systems. Study on the growth of gold nanoparticles was carried out separately using hydroquinone; green tea and chromium chloride respectively. We have reported the synthesis of gold nanoparticles of different shapes and sizes which was confirmed by different characterization techniques such as UV-visible, XRD, FESEM, DLS and Zeta potential analysis

Chapter 1

Iron Oxide Nanoparticles

1.1. INTRODUCTION

1.1.1: Superparamagnetism

The synthesis of superparamagnetic nanoparticles is gaining considerable importance in recent times because of their wide range of applications such as targeted drug delivery, MRI contrast agents, hyperthermia treatment for malignant or cancer cells, gene therapy etc. Most of the applications require the size of the nanoparticles to be smaller than 100 nm, typically as low as 10-20 nm[1]. Such narrow particle size distribution makes the nanoparticles behave as individual magnetic domain acting as 'single super spin' which accounts for their superparamagnetic behaviour. Such nanoparticles have high magnetization values and high magnetic susceptibility with minimal retentivity and coercivity[2]. These particles can easily bind to proteins, drugs and antibodies to be directed to target tissues or organs for its treatment by means of external magnetic field. Such nanoparticles have reduced risk of aggregation which accounts for its availability in wide range of applications. But the major problem associated with such nanoparticles is that they have high surface area to volume ratio which forces these particles to reduce their energy by forming agglomerates. Thus several protection strategies are employed to stabilize the nanoparticles by surfactant or polymer coatings, organic or inorganic layer coatings etc. Such functionalized nanoparticles are highly useful in applications related to catalysis, bio-sensing applications etc. Most of the commonly used magnetic nanoparticles include magnetite (Fe_3O_4) and maghemite (γ-Fe_2O_3). Both of them are ferromagnetic in nature but upon size reduction to 30 nm or less, they become superparamagnetic in nature by losing their permanent magnetism.

1.1.2: Structure and Magnetic properties

Magnetite (Fe_3O_4) exhibits an inverse spinel structure where Fe^{3+} ions occupies all the tetrahedral sites and both Fe^{3+} and Fe^{2+} ions occupies all the octahedral sites with oxygen forming FCC crystal system. In case of maghemite (γ-Fe_2O_3), there is random distribution of cations over 8 tetrahedral and 16 octahedral holes with Fe^{3+} ions occupying the tetrahedral sites and both Fe^{3+} ions and cationic vacancies occupying the octahedral sites [3].

Fe_3O_4: $[Fe^{3+}]_{Td}\,[Fe^{3+}, Fe^{2+}]_{Oh}\,O_4$

γ-Fe_2O_3: $0.75[Fe^{3+}]_{Td}\,[Fe^{3+}_{2/3}, V_{1/3}]_{Oh}\,O_4$

Presence of 4 unpaired electrons in 3d orbital of iron accounts for its strong magnetic moment. Fe^{2+} and Fe^{3+} ions have 4 and 5 unpaired electrons respectively in 3d shell. The net magnetization values of Fe_3O_4 and γ-Fe_2O_3 are calculated to be around 4.1 μ_B and 2.3 μ_B.

1.1.3: Synthesis of Magnetic Nanoparticles

Fe_3O_4 nanoparticles have been considered as interesting for the construction of organogels because of strong superparamagnetic property, low cost and biocompatibility. Numerous chemical methods have been used to synthesize magnetic nanoparticles for their usage in these applications such as Co-precipitation [4], Solvothermal method [5], hydrothermal reaction [6], sol gel synthesis [7], DC-thermal arc plasma method [8], etc. Among the various techniques, Sol-gel process holds several advantages over other methods in terms of greater homogeneity, large scale production at low cost [9]. The techniques employed for the synthesis of magnetic nanoparticles for preparing magneto-organogels is briefly discussed below.

1.1.3.1: Co-precipitation method

One of the simplest and effective chemical pathways to synthesize magnetic nanoparticles is the co-precipitation technique. Iron oxide nanoparticles are prepared by a stoichiometric mixture of Fe^{2+} and Fe^{3+} salts in aqueous medium at elevated or room temperature. The chemical reaction for this technique can be illustrated as-

$$\mathbf{FeCl_2\,(aq.) + 2\,FeCl_3\,(aq.) + 8\,MOH\,(aq.) \longrightarrow Fe_3O_4\,(s) + 8\,MCl\,(aq.) + 4\,H_2O\,(liq.)}$$

(M = Na^+, NH_4^+). Stoichiometric ratio of 2:1 (Fe^{3+}/Fe^{2+}) is used in an inert atmosphere and precipitation of Fe3O4 takes place when the pH of the solution comes in the range of 8 to 14.

Particle size gets smaller with the increase in pH and ionic strength of the medium. The main advantage of this technique is that it leads to the production of large quantity of nanoparticles [10]. Oxidation of magnetite nanoparticles leads to the formation of maghemite. Mean size of the particles can be controlled by adjustments in pH values and reaction temperature.

1.1.3.2: Thermal Decomposition method

Thermal decomposition of organometallic precursors in organic solvents having high boiling points along with surfactants leads to the synthesis of monodispersed magnetic nanoparticles. The organometallic compounds include metal acetylacetonates, metal carbonyls etc. Surfactants such as oleic acid and hexadecylamine are also used. Particle size and morphology is controlled by adjusting the ratios of starting materials as well as the reaction time and temperature. The rate of the reaction increases by reducing the chain length of fatty acids used as surfactant. Mono-dispersed nanoparticles in the size range from 4-10 nm have been successfully prepared by this technique [11]. Decomposition of $Fe(acac)_3$ in the presence of oleylamine and octadecene leads to the formation of iron oxide (Fe_3O_4) nanoparticles at 300°C with a heating rate of 20°C/min. Stabilization of nanoparticles is achieved by surfactant adsorption on the surface of iron oxide nanoparticles. This method is quite suitable for industrial preparation since high temperature and toxic reactants are involved [12].

1.1.4: Stabilization of Magnetic Nanoparticles

Effective chemical strategies are getting developed to prevent the aggregation of magnetic nanoparticles. Smaller size of the particles makes them highly sensitive towards oxidation. Most of the protection strategies involve coating of the nanoparticles with surfactants, polymer and inorganic layer of components [13, 14]. The impenetrable layer created across the surface of nanoparticles prevents the particles from coming in contact with oxygen. The major stabilizing agents are listed below –

- Monomeric stabilizers: Phosphates, Carboxylates.
- Inorganic materials: Silica, Gold, Silver, Carbon.
- Polymer stabilizers: Dextran, Polyethylene glycol(PEG), Polyvinyl alcohol(PVA), Alginate, Chitosan.

In this project work, stabilization of magnetic nanoparticles is achieved by using phosphatidylcholine for the synthesis of magnetoliposomes and by using oleylamine for the synthesis of magneto-organogels. In the latter case, oleylamine serves both the functions of preventing the agglomeration of nanoparticles as well as making the magnetic nanoparticles soluble in organic mediums such as hexane, chloroform etc suitable for synthesizing magneto-organogels.

1.1.5: Magneto-Liposomes

Liposomes are lipid-based nanoparticles used extensively in the pharmaceutical and cosmetic industries because of their capacity for breaking down inside cells, once their delivery function has been met. Liposomes were the first engineered nanoparticles used for drug delivery but problems such as their propensity to fuse together in aqueous environments and release their payload, have led to replacement, or stabilization using newer alternative nanoparticles. Magnetoliposomes are the magnetic nanoparticles coated in a lipid bilayer and they provide a highly flexible system for biocompatibility, chemical functionality and drug delivery resulting in synergistic treatment strategy [15]. Since the properties of lipid bilayer are mostly dependent on temperature, these Magnetoliposomes are considered to be useful for hyperthermia [16]. Magnetite is an ideal candidate material for the core of magnetoliposomes. Being superparamagnetic in nature, it has a lower stray magnetic field intensity in comparison to ferromagnetic materials. This lower field is beneficial because it reduces the potential health risks posed by weak magnetic fields. In addition to that, these materials have lower chance of agglomeration than ferromagnetic materials due to magnetostatic interactions. In this project work, magnetoliposomes have been developed by stabilizing the magnetite nanoparticles synthesized through the co-precipitation method with soybean phosphatidylcholine (SPC) since it contributes to stop the nanoparticles from growing too large.

1.1.6: Magneto-organogels

In general, gels contain two components, one of which is a liquid and the other, a solid. The solid components form a three-dimensional networked structure which helps in immobilizing the liquid component. The solid components are often regarded as gelators. Depending on the

polarity of the liquid component, the gels may be regarded either as hydrogels (Polar phase) or Organogels (apolar phase). The immobilization of the liquid within the three-dimensional network structure has been attributed to the surface active phenomena amongst the solid and the liquid phases. As the name organogels suggests, organogels contain apolar solvents (e.g. kerosene oil, sunflower oil, mustard oil, mineral oil) as the continuous phase. Organogels are semi-solid systems in which a three-dimensional network of gelator molecules or aggregates immobilizes an organic liquid continuous phase, typically an apolar solvent or oil [17]. The skeleton of the gelled structure consists of either polymers or low molecular weight organogelators. These form a cross-linked structure either by physical or chemical interactions, thereby immobilizing the organic phase within the network. Molecular interactions such as hydrogen bonding, metal coordination or dipolar interactions are responsible for the organogels structure [18]. Organogels are viscoelastic systems, having both viscous and elastic properties.

Gels sensitive to magnetic fields are of interest as smart materials. They have novel potential applications in sensors, controlled delivery systems, separation systems and artificial muscles. Typically, magneto sensitive gels are polymer gel systems with a polymer framework sustaining solution containing magnetic nanoparticles. Since magnetic nanoparticles are responsive to magnetic field stimuli, changes such as gel breakage or shrinking can be expected to occur to this system under the application of an external magnetic field. Such a system can be adjusted to be a magneto-sensitive gel, and this might have potential applications in sensors and controlled release systems. In this project work, two types of magneto-organogels have been prepared and characterized where one was synthesized using stearic acid and oleic acid while the other was prepared using stearic acid and soybean oil. Stearic acid offers the possibility of additional intermolecular interactions (H bonding) within the low molecular mass organic gelator assemblies. Organogels containing oleic acid holds potential for use as rectal sustained release preparation. But the stearic acid and oleic acid based magneto-organogels being unstable were discontinued for further characterization while the work proceeded with the stearic acid and soybean oil based organogels.

1.2. EXPERIMENTAL

1.2.1: Synthesis of magnetic nanoparticles by co-precipitation method

Materials: Ferrous chloride anhydrous ($FeCl_2$) (AR grade, Nice Chemicals Pvt. Ltd.) and ferric chloride hexahydrate ($FeCl_3.6H_2O$) (AR grade, LOBA chemicals) were used as the precursors for the co-precipitation method. Ammonium hydroxide (25 wt% NH_3 in water) (AR grade, sd fine-chem limited) was used as the precipitating agent. All of the materials were used without further purification. Water was deionized prior to use.

Synthesis of the magnetic nanoparticles by co-precipitation method: The magnetic nanoparticles were prepared via the chemical co-precipitation method by taking 124.5 mg of $FeCl_2 \cdot 4H_2O$ and 202.5 mg of $FeCl_3$, with the molar ratio of ferric ion to ferrous ion in the solution of 1.63, were dissolved in 150 ml of deionized water (maintained at pH=1.5) under a nitrogen gas flow with vigorous stirring at room temperature for about 20 minutes. A 10 ml of 25 wt% NH_4OH (excess base concentration) was carefully added to the solution dropwise till the pH of the solution reached 9.0 from 1.5, and then the solution colour changed from orange to black rapidly. The magnetic nanoparticles were separated by magnetic decantation and thoroughly washed with deionized water to remove chloride ions and then washed with ethanol several times to remove excess of ammonia and finally freeze-dried by lyophilizer for 48 h. The bare magnetic nanoparticles were prepared by this procedure.

1.2.2: Synthesis of oleylamine coated magnetic nanoparticles by thermal decomposition method

Materials: Iron(III) acetylacetonato ($Fe(acac)_3$) (AR grade, Sigma–Aldrich), 1-octadecene (AR grade, Sigma–Aldrich) and oleylamine (AR grade, Sigma–Aldrich), were used as the precursors for the thermal decomposition method. All of the materials were used without further purification.

Synthesis of the oleylamine capped magnetic nanoparticles (MNPs): Oleylamine coated Fe_3O_4 nanoparticles were prepared following a published procedure [12] with some modifications. In the first step, 530mg of $Fe(acac)_3$ was dissolved in 7.5 mL of 1-octadecene and 7.5 mL of oleylamine. The solution was dehydrated at 110°C for 1 h under vacuum. The reaction vessel was filled with nitrogen and quickly heated to 300 °C at a gradual increase in the heating rate.

The reaction was continued for 1 h at this temperature. After the reaction, the solution was cooled down to room temperature. The Fe_3O_4 nanoparticles were washed twice with 30 mL of ethanol, followed by centrifugation at 3500rpm for 10 minutes and later dispersed in chloroform at room temperature for further use.

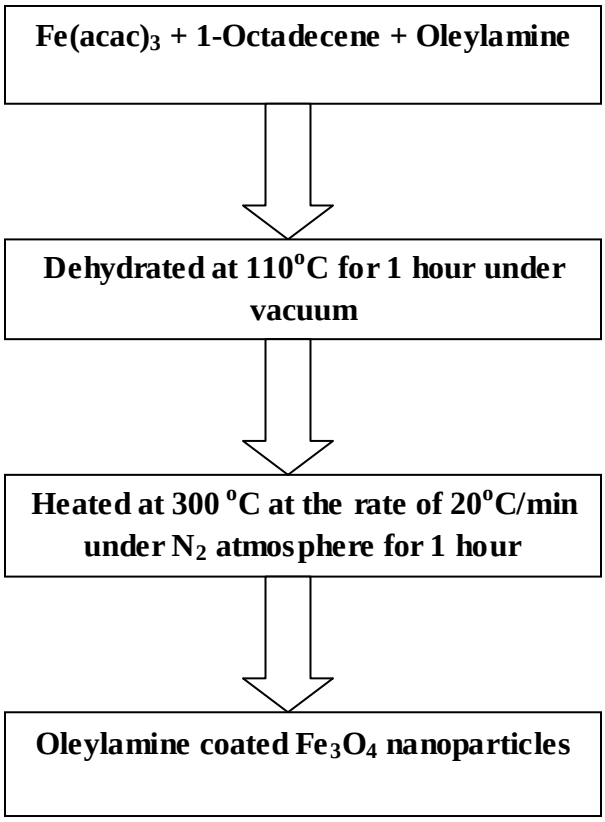

Figure 1: Scheme for synthesis of oleylamine coated Fe_3O_4 nanoparticles

1.2.3: Synthesis of magneto-liposomes

Materials: Ferrous chloride anhydrous ($FeCl_2$) (AR grade, Nice Chemicals Pvt. Ltd.) and ferric chloride hexahydrate ($FeCl_3.6H_2O$) (AR grade, LOBA chemicals) were used as the precursors for the co-precipitation method. Ammonium hydroxide (25 wt% NH_3 in water) (AR grade, SD fine-chem limited) was used as the precipitating agent. Soybean lecithin (HI-MEDIA) was used for coating magnetite nanoparticles. All of the materials were used without further purification. Water was deionized prior to use.

Synthesis of magneto-liposomes: The first step in the synthesis is the preparation of Ferrofluid which involves the addition of a solution of soy lecithin in methanol to the solution of $FeCl_2$ and $FeCl_3$ in a molar ratio of 1:2 in water (0.2 M). A 10 ml of 25 wt% NH_4OH (0.93 M) was carefully added to the solution dropwise till the solution colour changed from orange to black rapidly. The solution was kept at magnetic stirring under nitrogen gas flow for further 15 minutes. The phosphatidylcholine coated magnetic nanoparticles were separated by magnetic decantation and thoroughly washed with deionized water to remove chloride ions and then washed with ethanol and acetone several times to remove excess of ammonia and finally freeze-dried by lyophilizer for 48 h. Soy lecithin (190 mg) was dissolved in chloroform (10 ml) and was dried in a rotary evaporator under reduced pressure at 40 °C to yield a lipid film. The lipid film was then hydrated with the aqueous solution of Ferrofluid (1.25 mg of PC coated magnetite in 50 ml H_2O) for 24 hr after which it was subjected to bath sonication for 10 minutes to obtain magneto-liposomes.

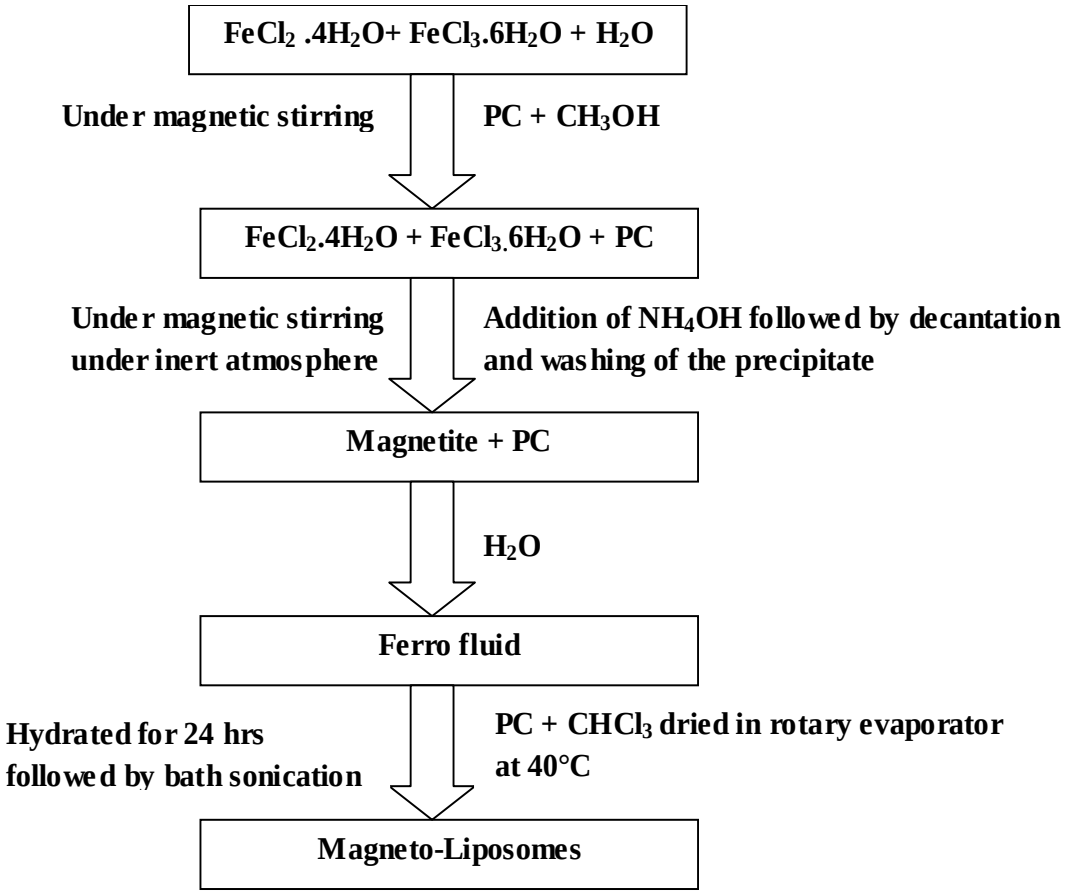

Figure 2: Scheme of formation of magneto-liposomes

1.2.4: Synthesis of Magneto-organogels using oleylamine coated Fe_3O_4 nanoparticles

Materials: Stearic Acid ($C_{18}H_{36}O_2$) and Oleic Acid ($C_{17}H_{33}COOH$) were purchased from HI-MEDIA. Soybean oil was commercially available and used as received.

(a) Preparation of Organogels (Stearic acid + Oleic acid): The organogels were developed by varying the proportions of stearic acid and oleic acid. The proportion of stearic acid was varied from 5- 30% (w/w) of the total organogel amount. The samples were prepared by dissolving specific weight of stearic acid in oleic acid kept in a water bath at 70^{o}C until a homogeneous solution was obtained. The solution, so obtained was allowed to cool down to room temperature. The critical gelling concentration (CGC) of stearic acid was determined. The magneto-organogels samples were prepared by adding different amounts of oleylamine coated Fe_3O_4 nanoparticles at CGC and repeating the above procedures. The samples were stored at room temperature for further analysis.

(b) Preparation of Organogels (Stearic acid + Soybean oil): Organogels of various compositions were prepared by dissolving specific amount of stearic acid, kept in a water bath maintained at 70^{o}C until a clear homogeneous solution was obtained. The proportion of stearic acid was varied from 10-20 % (w/w). The hot solution so obtained was allowed to cool down at room temperature so as to allow gel formation. The samples were regarded as organogels, if upon cooling, the solution mixture failed to flow when the culture bottles were inverted. The CGC of stearic acid was determined. Oleylamine coated Fe_3O_4 nanoparticles were introduced at the CGC and the magneto-organogels samples were prepared using the above procedure. All the samples were kept at room temperature for further analysis.

Accurately weighed stearic acid was dissolved in oleic acid at 70^{o}C. The concentration of stearic acid was varied from 5% to 30% (w/w) in order to determine the critical gelling concentration (CGC). The hot stearic acid solution was subsequently cooled down at room temperature. The precipitation of stearic acid molecules made the solution cloudy. Depending on the concentration of stearic acid in oleic acid, the solution either remained cloudy or formed an opaque solid like structure. The samples were regarded as organogels, if the final product did not flow when the culture bottles were inverted. The CGC of stearic acid to immobilize oleic acid was found to be 16% (w/w). Similar procedure was adopted for stearic acid-soybean oil based organogels were the CGC was determined to be 10% (w/w).

Varying compositions of oleylamine coated Fe_3O_4 nanoparticles were introduced at the CGC for both the kinds of organogels and the samples were prepared using the same procedure as given above. The composition of the organogels which were used for further analysis has been tabulated in Table. It was observed that the organogels with higher proportions of stearic acid attained the gel structure relatively quickly.

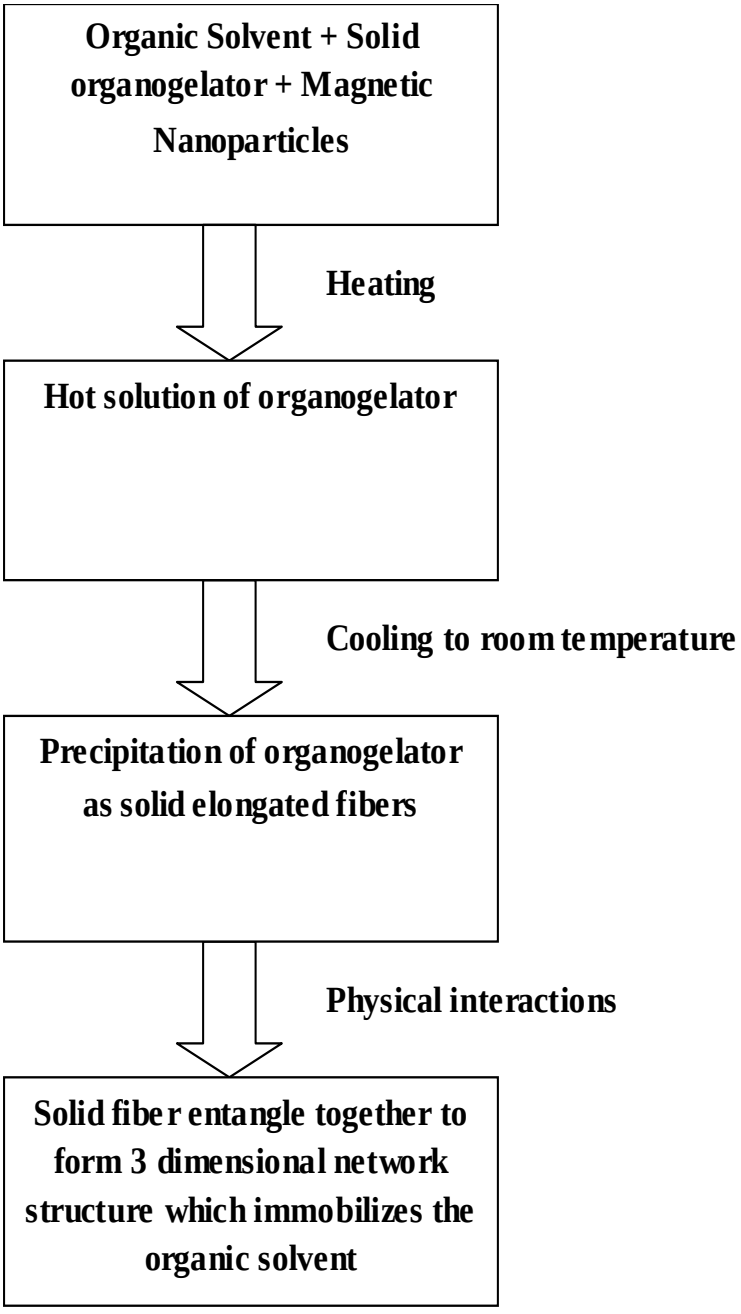

Figure 3: Scheme of formation of magneto-organogels

Table 1: Composition of stearic acid and oleic acid used for the determination of CGC

Sample	Concentration of various components (%, w/w)	
	Stearic Acid	Oleic Acid
S1	5	95
S2	10	90
S3	11	89
S4	12	88
S5	13	87
S6	14	86
S7	15	85
S8	16	84
S9	20	80
S10	25	75
S11	30	70

Table 2: Composition of magneto-organogels (using oleic acid) selected for further analysis (10 g of organogel)

Sample	Concentration of various components		
	Stearic acid (in g)	Oleic acid (in g)	Magnetic nanoparticles (in mg)
Control	1.6	8.400	-
M1	1.6	8.395	5
M2	1.6	8.390	10
M3	1.6	8.385	15
M4	1.6	8.380	20

Table 3: Composition of magneto-organogels (using soybean oil) for further analysis (10 g of organogel)

Sample	Concentration of various components		
	Stearic acid (in g)	Oleic acid (in g)	Magnetic nanoparticles (in mg)
S10	1.0	9.0000	-
S20	2.0	8.0000	-
M10	1.0	8.9995	0.5
M20	2.0	7.9995	0.5

Images of the organogels and magneto-organogels synthesized as reported in the tables given above:

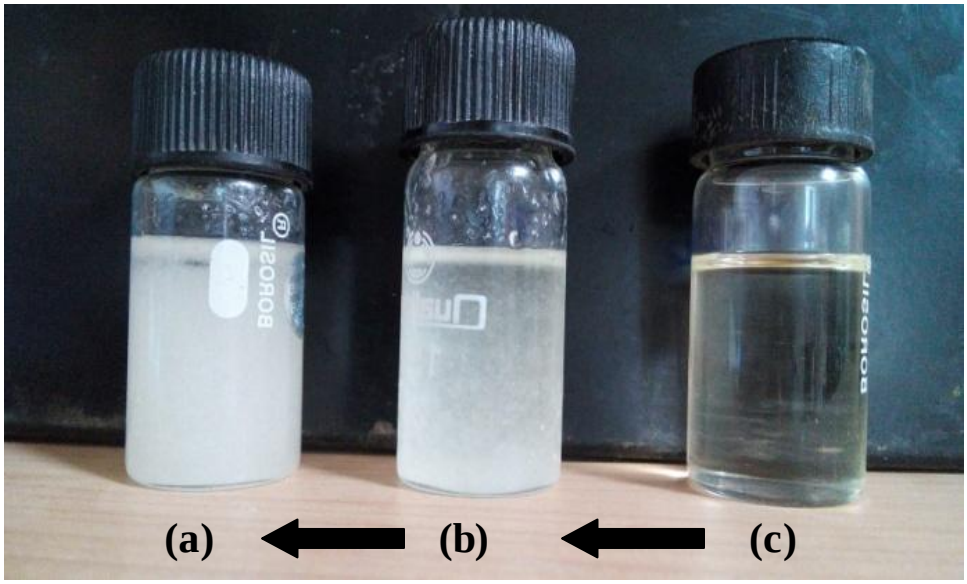

Figure 4: Gelation process of organogel using oleic acid from (c) to (a) where (c) clear solution after heating (b) uniform cloudy suspension after cooling and standing (a) opaque semi solid gel upon further standing.

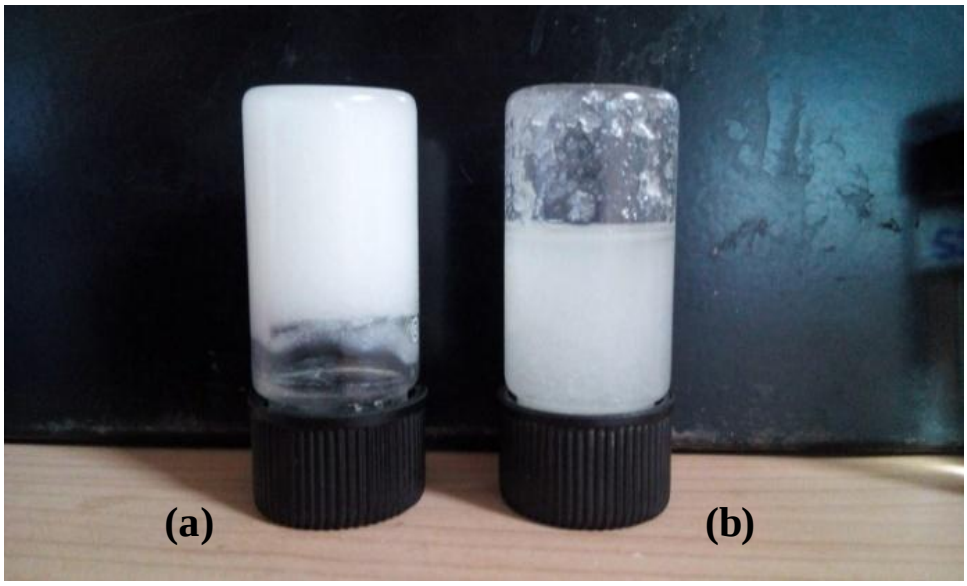

Figure 5: Upon cooling and standing (a) formed organogel (b) failed to form organogel as the suspension flows on inverting the culture bottle.

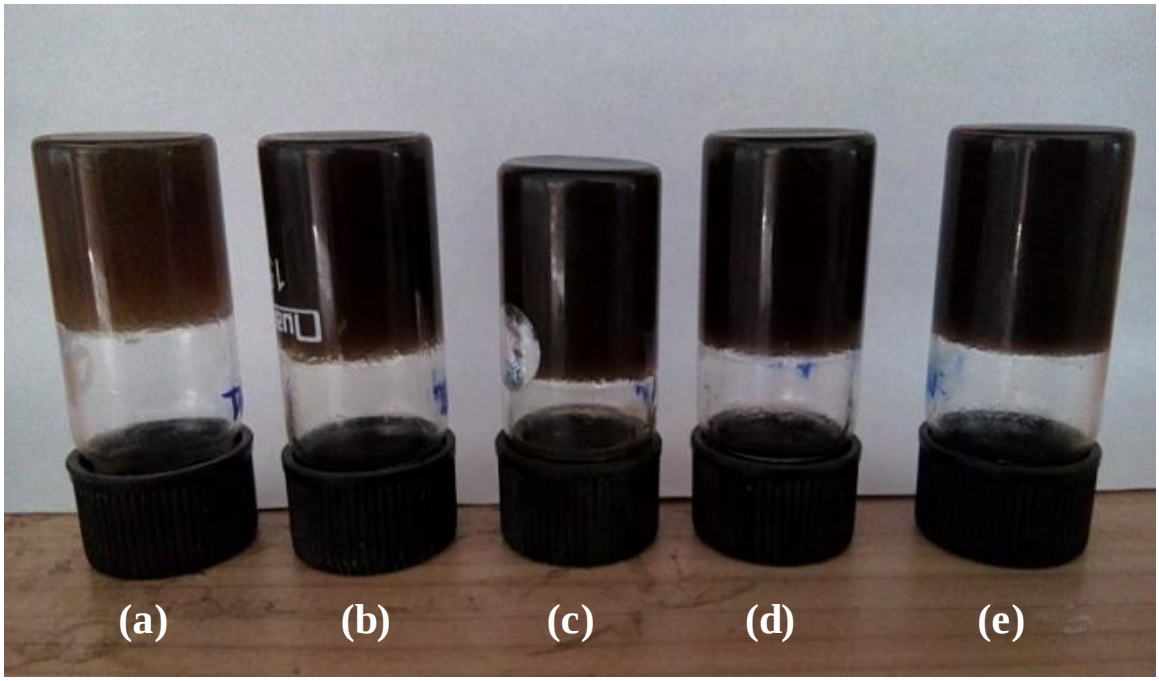

Figure 6: Magneto-organogels formed using oleic acid containing oleylamine coated Fe_3O_4 NPs in the amount of (a) 5 mg (b) 10 mg (c) 15 mg (d) 20 mg (e) 25 mg

(a) (b) (c) (d)

Figure 7: Magneto-organogels synthesized by adding oleylamine coated Fe_3O_4 NPs to stearic acid and oleic acid (a); (b) and to stearic acid and soybean oil (c); (d).

1.3. RESULTS AND DISCUSSION

1.3.1: *Characterization of the bare Fe_3O_4 magnetic nanoparticles (MNPs) and Oleylamine capped Fe_3O_4 magnetic nanoparticles:*

The magnetic nanoparticles and oleylamine capped magnetic nanoparticles (MNPs) were first characterized for the functional groups by a FT-IR spectrometer (Perkin-Elmer) in the absorption mode. A wide angle X-ray diffractometer (Rigaku) with Cu K_α source was used to study the crystalline structure of the magnetic which was below the nanometer scale. For X-ray analysis, the magnetic nanoparticles were placed into a sample holder and the measurement was continuously run. The experiment was recorded by monitoring the diffraction pattern appearing in the range from 20 to 70 with a scan speed 1°/min and a scan step 0.02°. A scanning electron microscope FEI-FESEM (Nova nano SEM) operated at 5 kV was used to examine the morphological structure and to measure the particle size of the magnetic nanoparticles.TGA was carried out using STA449C/4/MFC/G/ Netzsch, Germany at heating rate of 10°/min in presence of air atmosphere and a complementary argon flow was used as a protective gas.

1.3.1.1: XRD Analysis

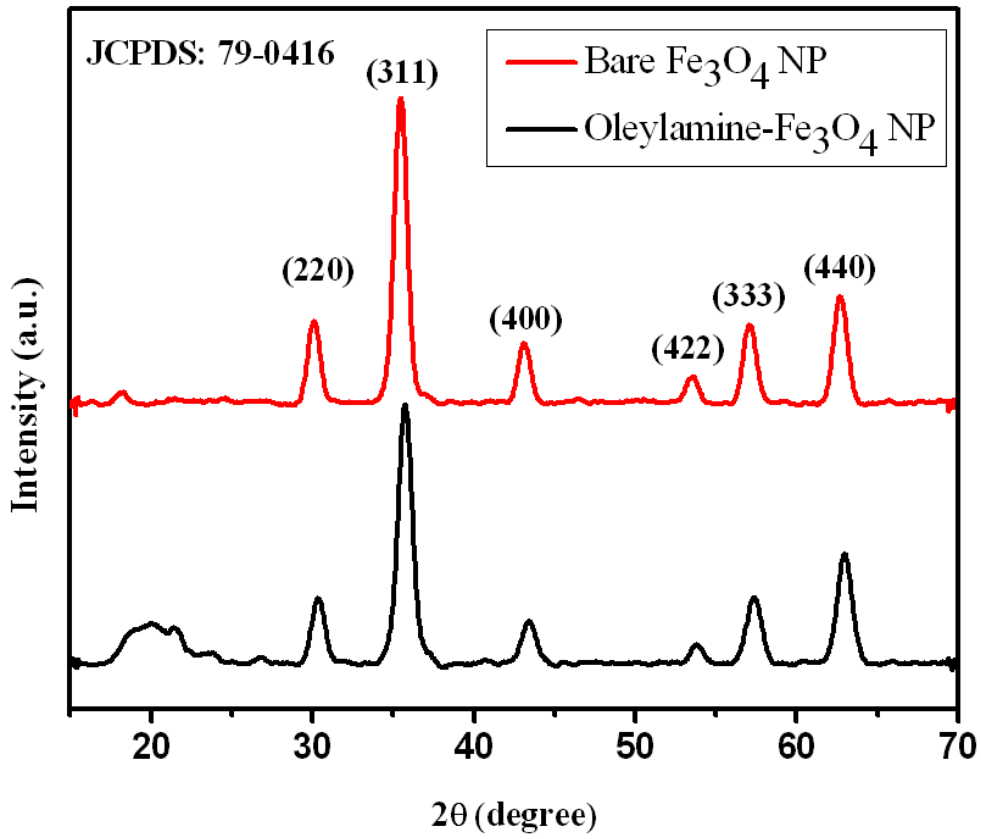

Figure 8: XRD pattern of (a) bare Fe_3O_4 NPs and (b) Oleylamine coated Fe_3O_4 NPs

The diffraction peaks of (220), (311), (400), (422), (511) and (440) reflect the magnetic crystal with a cubic spinel structure which corresponds to the available JCPDS data (JCPDS no.79-0416) for the bare Fe_3O_4 as well as for oleylamine capped Fe_3O_4magnetic nanoparticles (Fig.8). All the diffraction peaks of the bare Fe_3O_4 nanoparticles can be indexed to a pure, well crystalline, face centred cubic spinel structure. There is no other impurity peaks observed, indicating the high phase purity of cubic Fe_3O_4. The good crystallization is proved by its strong and sharp reflection peaks. Comparing the bare magnetite nanoparticles with the coated one, the XRD patterns show similar diffraction peaks; this indicates that the coating agent does not significantly affect the crystal structure of the magnetite nanoparticles.

1.3.1.2: FESEM Analysis

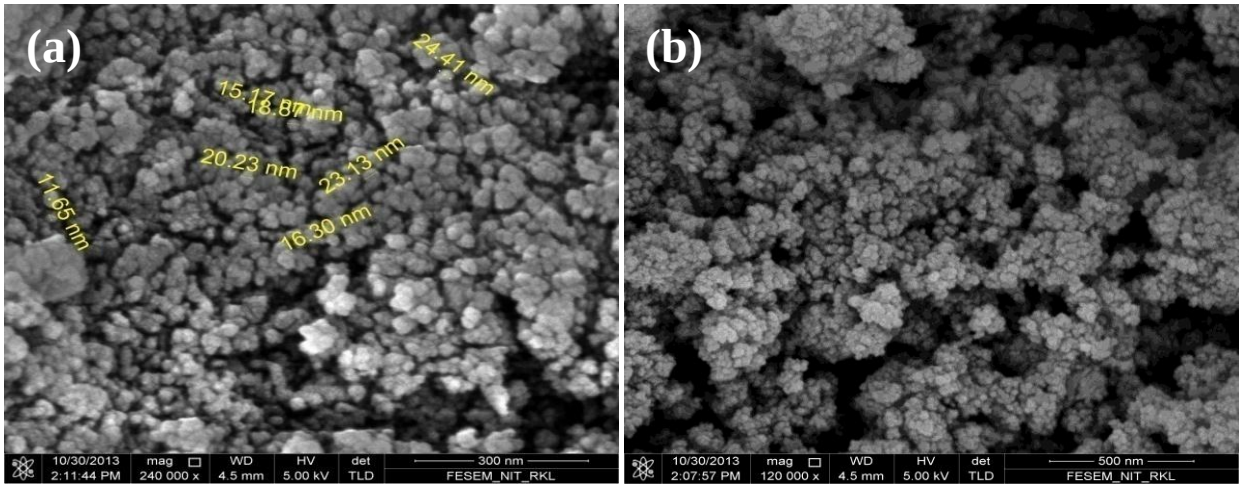

Figure 9: FESEM images of (a) bare Fe_3O_4 NPs and (b) Oleylamine coated Fe_3O_4 NPs

The spherical shaped nano size magnetic particles were successfully prepared as shown in fig.9. The SEM image of the bare magnetic and oleylamine capped MNPs are shown in Fig.9 (a) and 9(b) respectively. The bare Fe_3O_4 nanoparticles have a narrow size distribution with an average diameter of 20 nm; however, the particles tend to agglomerate when bare and left uncapped. The coating agent provided larger particle sizes due to the combination of the coating agent layer on the surface of magnetite. The size distribution pattern indicated polydisperse nanoparticles mostly in the size range of 25 to 35 nm as shown below (Fig.10)

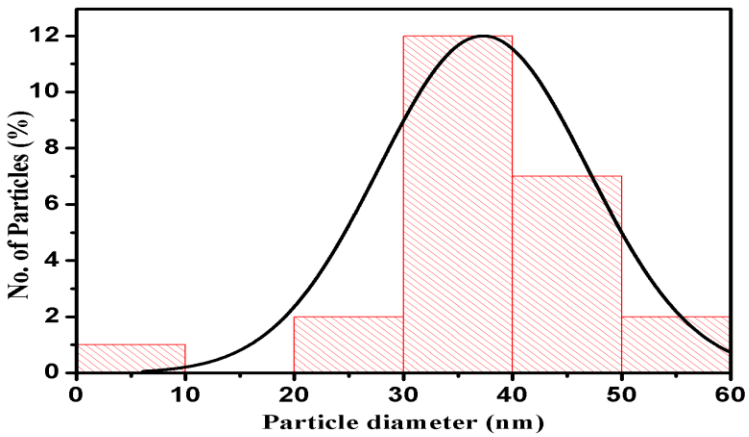

Figure 10: Size distribution pattern of Fe3O4 NPs

1.3.1.3: FTIR Analysis

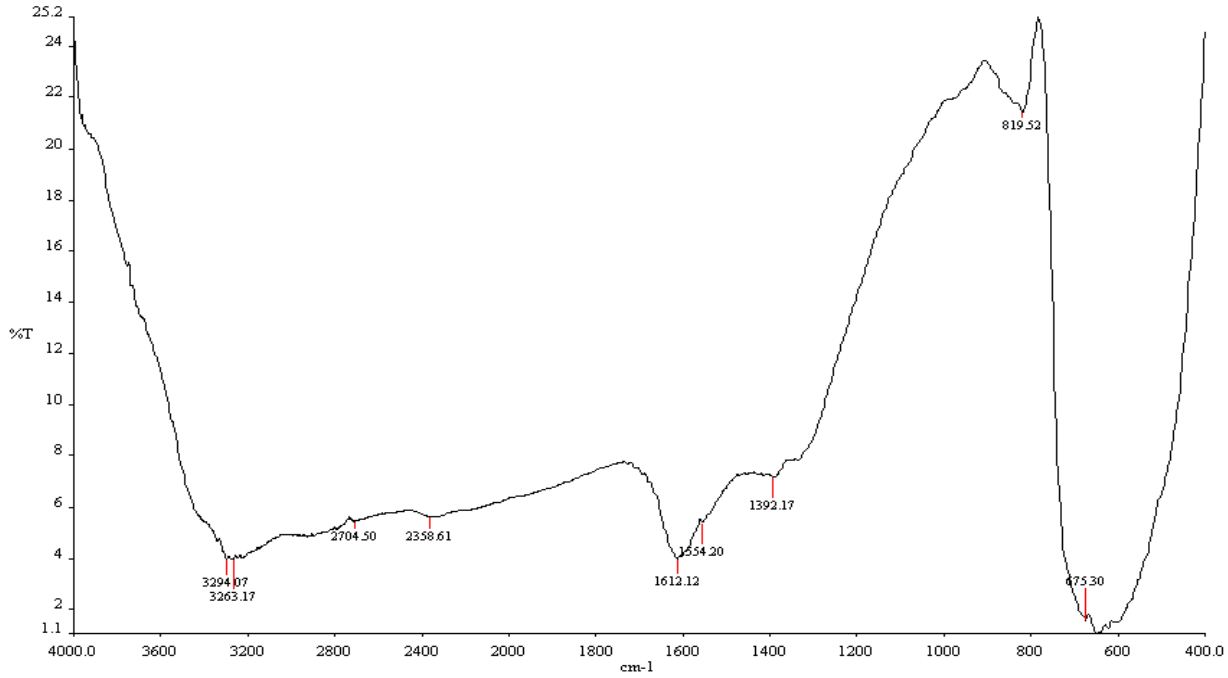

Figure 11: FTIR Spectrum of Fe_3O_4 NPs synthesized from co-precipitation method

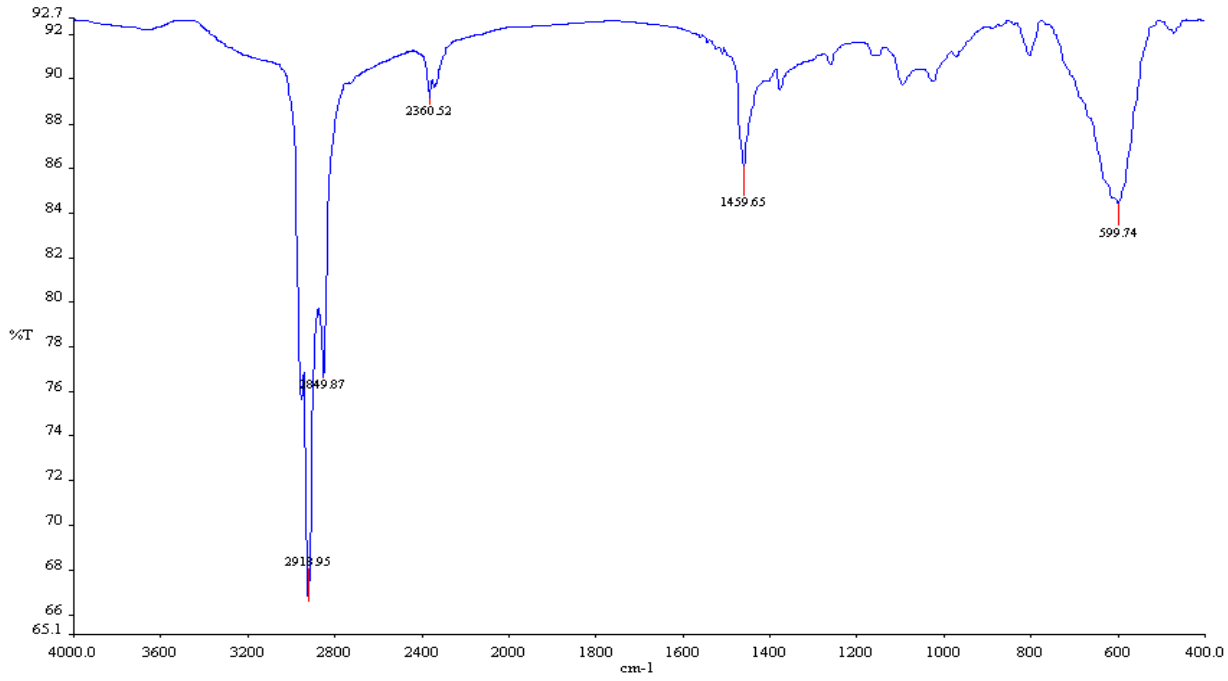

Figure 12: FTIR Spectrum of oleylamine coated Fe_3O_4 NPs

FTIR spectra of the bare magnetic nanoparticles and the oleylamine capped magnetic nanoparticles are shown in (Fig.11 and 12). For the magnetic nanoparticles, the band at around 600 cm^{-1} corresponds to the vibration of the Fe-O bonds. The crystalline structure of the magnetic nanoparticles is characterized by XRD as shown in Fig.8. The presence of oleylamine coating around the MNPs was confirmed by FTIR spectroscopy, where the sharp peaks at around 2900 cm^{-1} and 1050 cm^{-1} represented C-H and C-N stretching peaks, respectively (Fig.12). Those peaks are characteristic to oleylamine functionality.

1.3.1.4: Thermo Gravimetric Analysis (TGA)

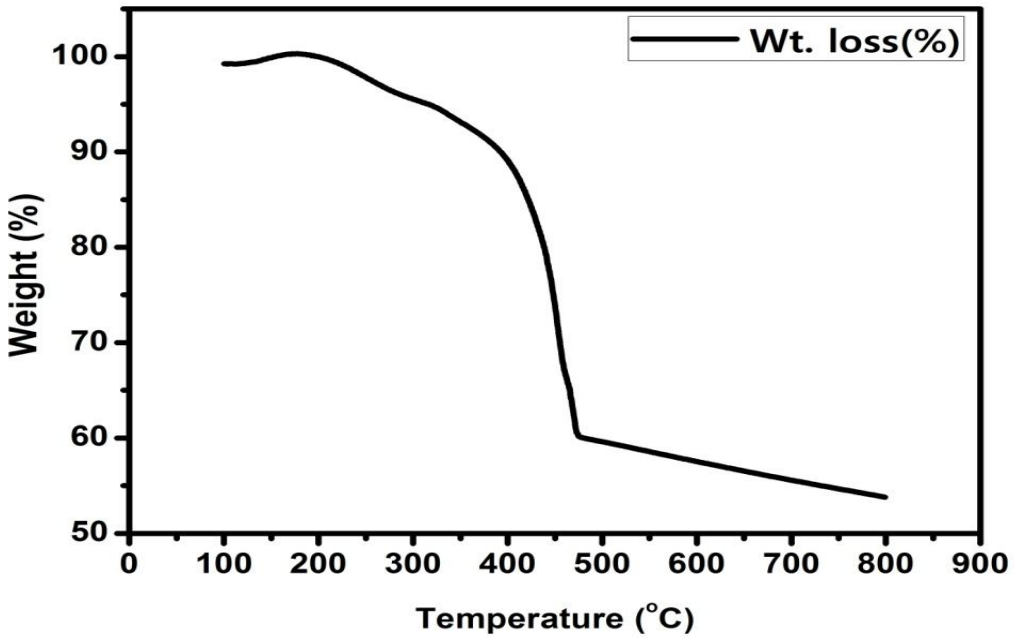

Figure 13: Thermal stability of the synthesized magnetic nanoparticles coated with oleylamine

The thermogram of the oleylamine coated magnetite nanoparticles is shown in Fig. 13. From the figure it is quite evident that the oleylamine coated magnetic nanoparticles are quite stable upto temperatures as high as 350 ^{o}C. The initial weight loss at temperature below 400^{o}C refers to the evaporation of oleylamine. The increase in weight loss around 500 ^{o}C corresponds to the complete loss of oleylamine capping and possible transformation of the magnetite to the hematite.

1.3.2: *Characterization of magneto-organogels:*

1.3.2.1: Microscopic Studies

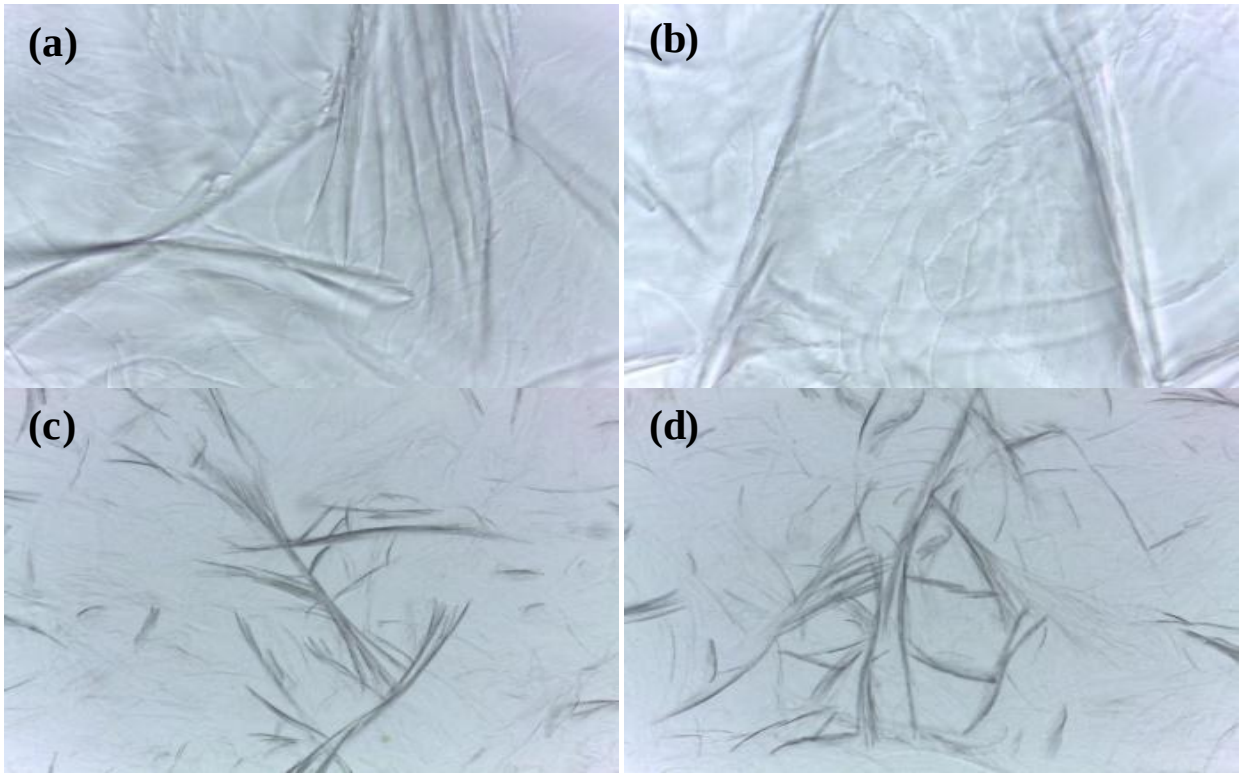

Figure 14: Micrographs of magneto-organogels synthesized using soybean oil and stearic acid at (a) Molten condition; t=0 (b) t=1 min (c) 10% (w/w) gelator (d) 20% (w/w) gelator

The process of gelation was monitored under a compound light microscope as the stearic acid solution in soybean oil is cooled at room temperature (figure 14(a); (b)). This was done to understand the underlying phenomena of gel formation. The micrographs showed the presence of gelator molecules dispersed in the liquid phase. The gelator molecules self-assemble into aggregates as the sample cools down. These clusters of gelator molecules resemble fiber-like structures. This solid skeleton of gelator aggregates is responsible for immobilizing the liquid phase and giving rise to a gel.The microstructure of the organogels showed the presence of fiber shaped crystals of stearic acid in soybean oil when 10% (w/w) gelator concentration was used (figure 14 (c)). As the concentration of the gelator was increased, these clusters aggregated to form fiber-like structures. The density of these fiber-like structures increased with the increase in the gelator concentration (figure 14(d)).

1.3.2.2: XRD Analysis

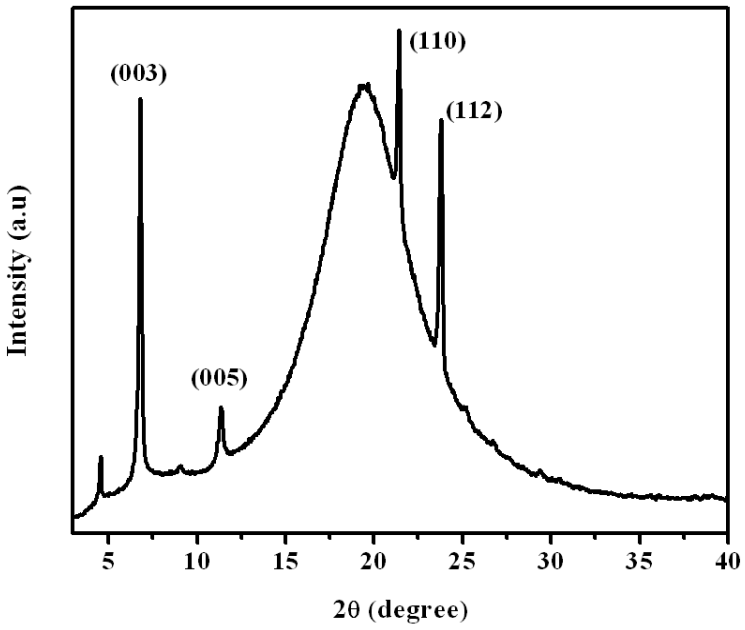

Figure 15: XRD pattern of soybean oil based organogel containing 10% (w/w) gelator

The position and *d*-spacing of the major peaks corresponding to stearic acid were conserved in the organogels [19] .This suggests that the polymorphic form of stearic acid was not altered during the formation of organogels. The intensity of the short spacing peaks were higher than the long spacing peaks. This suggested that the addition of soybean oil in the stearic acid resulted in the rearrangement of the molecular packing of stearic acid. The ratios of position of the 1st (6.89º 2θ), 2nd (11.5º 2θ) and 3rd (21.37º 2θ) low angle peaks of the gels with respect to lowest angle peak position (6.89º 2θ) was studied to identify the packing of gelator molecules [20]. XRD profiles of the developed gels showed that the ratios were nearly 1:1, 2:1 and 3:1, respectively. This type of arrangement supports the layered packing of stearic acid molecules in the organogels [20]. The amorphous peak (19.5º 2θ) associated with the XRD profile of the organogels was due to the presence of liquid triacylglycerols in soy bean oil.

1.3.2.3: FTIR Analysis

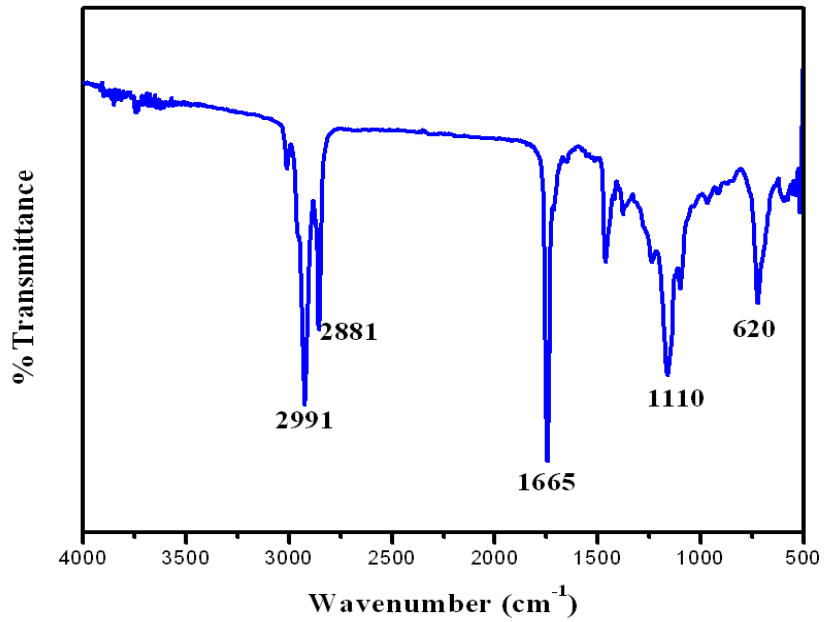

Figure 16: FTIR Spectra of soybean oil based organogel containing 10% (w/w) gelator

The possible chemical interactions for the lamellar arrangement of the stearic acid molecules were explained by the FTIR studies. FTIR spectrum of stearic acid shows its characteristic bands at ~1665 and 1110 cm^{-1} [22]. The bands at 1665 cm^{-1} and 1110 cm^{-1} were due to the stretching vibration of carbonyl group and bending vibrations of hydrogen bond (OH-H) involving carboxylic acid, respectively. The band at around 600 cm^{-1} corresponds to the vibration of the Fe-O bonds of magnetite nanoparticles while the sharp peaks at around 2991 cm^{-1} and 1050 cm^{-1} represented C-H and C-N stretching peaks, respectively The characteristic peaks of stearic acid were retained in the FTIR spectra of the organogels. The characteristic peaks of stearic acid were shifted towards lower wave number in the organogels. This may be due to the involvement of the carboxylic group of stearic acid in the non-covalent interactions (hydrogen bonding) during gelation. Gelator-solvent interactions also might have contributed to the shifting of the bands in the organogels. Fatty acids present in soy bean oil have been involved in the formation of hydrogen bonds with the stearic acid molecules. This resulted in the incorporation of the soybean oil within the lamellar structure of the stearic acid.

1.3.2.4: DSC Analysis

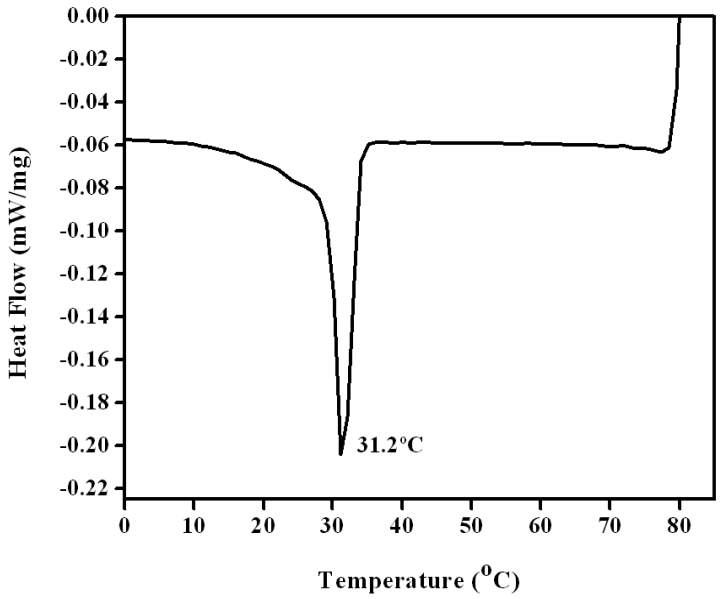

Figure 17: DSC thermogram of soybean based organogel containing 10% (w/w) gelator

Melting behavior of stearic acid and organogels was tested below 100 ºC. The sample 10% (w/w) organogel was subjected to thermal analysis, using a differential scanning calorimeter, in the temperature range of 29°C to 80°C. Characteristic endothermic peaks were observed in DSC thermograms. The results indicate that the additional/excess heat involved (apart from fiber melting) during the phase change might have contributed to the dissolution of the fibers (fibrous structure of the organogel reported in the microscopic studies).

1.3.2.5: Impedance Analysis

The detailed impedance analysis and calculations of the soybean oil based organogels is still underway and is likely to contribute a great deal towards the future scope of this study of magneto-organogels. From the preliminary analysis, magneto-organogels have been found to be conducting even at low concentrations (0.5 mg) and is found to have low impedance (resistance) which can be used in the application of controlled drug release by the electro-responsive nature of the gel.

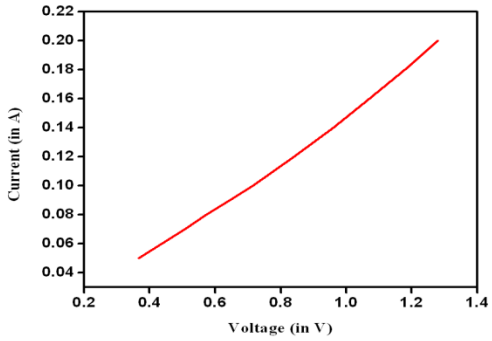

Figure 18: V-I curve for soybean oil based organogels

1.3.2.6: FESEM Analysis

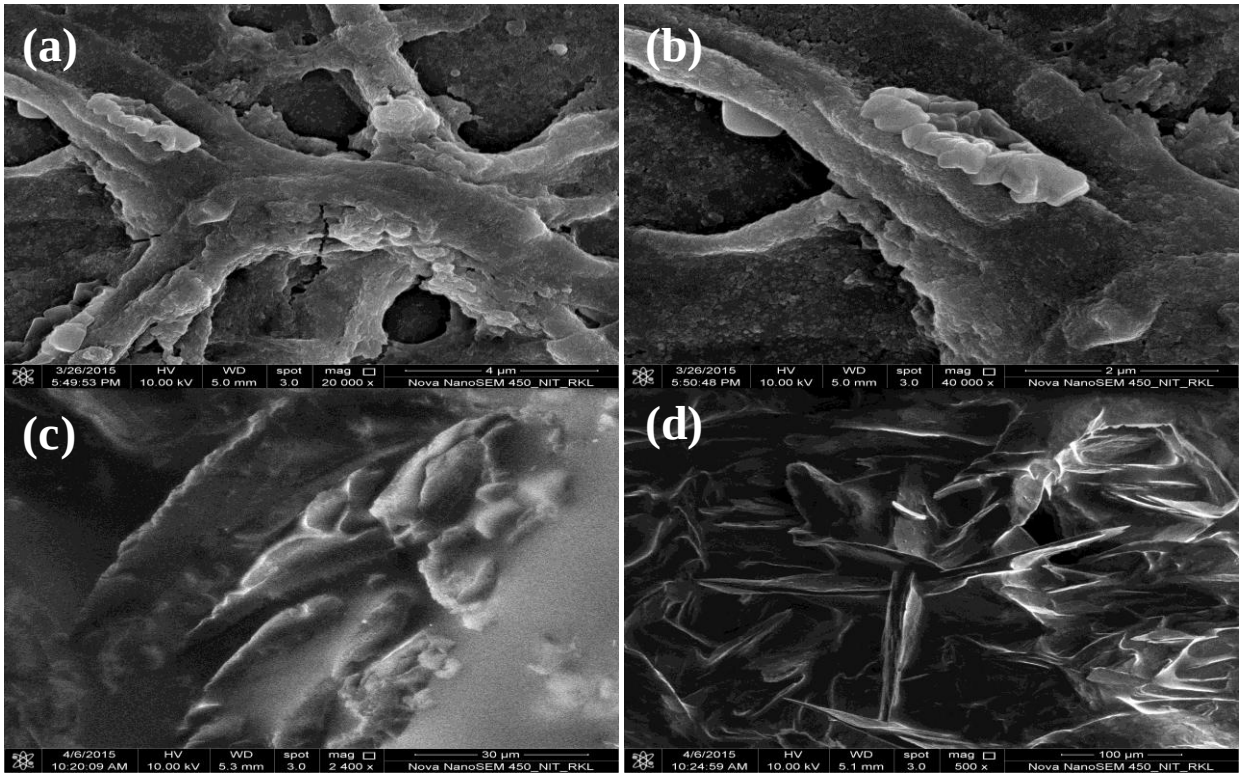

Figure 19: FESEM images of oleic acid based organogel (a); (b) and soybean oil based organogel containing (a) 10% gelator (b) 20 % gelator

Typical FESEM images displayed above represents the three dimensional networked structure of gelator framework.These aggregates form a three-dimensional network which is responsible for immobilizing the solvent. The rod like tubular structures displayed in the images can help in entrapping the magnetic nanoparticles within its framework.

1.3.2.7: Release kinetics study of Rhodamine-B dye in organogels

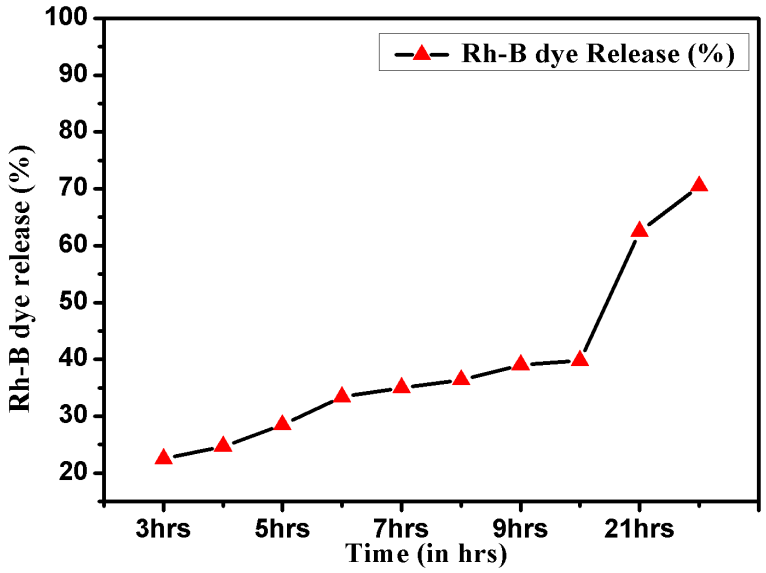

Figure 20: Rhodamine-B dye release profile of organogel containing 10% gelator

In the release experiment, the Rh-b dye loaded organogel (450 mg) was suspended in 3 ml of PBS buffer solution (pH 7.4). The suspensions were transferred into a dialysis bag (Mw = 14000) and placed in a beaker containing 100 mL of buffer at the same pH condition. At fixed time intervals, 1 mL of solution was withdrawn while the same volume of fresh corresponding buffer maintained at same condition was added to the original suspension. The amount of Rh-B dye release was determined by UV−visible spectroscopy.The release profiles of the dye from the organogels have been shown in figure 20. The initial low % release value indicates the controlled release behavior of the formulation. The amount of dye release from the as prepared magneto-organogel was found to be 70 % (approx.) after 30 hrs. For release studies, we used Rh-B dye as a model to mimic the drug situation in PBS buffer (pH = 7.4) to load the dye molecules in as prepared magneto-organogel. At the end of the loading procedure, we found an appreciable difference of absorbance values of Rh-B dye in the solution before and after the dye loading experiment. The release studies of the dye indicated that the organogels may be used as matrix for controlled delivery systems. This result supports our hypothesis of trapping of drugs inside the matrix of organogel.

1.4. CONCLUSIONS

The magnetic nanoparticles are successfully synthesized in range of 10–40 nm yielding excellent magnetic properties. The co-precipitation method of synthesis produces the spherical-shaped morphology of magnetic nanoparticles. Oleylamine coated Fe_3O_4 nanoparticles have been synthesized by thermal decomposition method. The synthesized particles were first characterized by Field Emission Scanning Electron Microscopy (FESEM). The average size of the particles was found be around 20 nm (Fig.9). The dried powder of the material has been shown to hold a permanent magnet (NdFeB) freely. The presence of oleylamine coating around the MNPs was confirmed by FTIR spectroscopy, where the sharp peaks at around 2900 cm^{-1} and 1050 cm^{-1} represented C-H and C-N stretching peaks, respectively (Fig.12). All these characterization data indicate the successful synthesis of oleylamine coated Fe_3O_4 magnetic nanoparticles with an average size of 20 nm that are readily dispersed in organic solvent like chloroform, hexane, DCM etc. for further use.

Organogels with varying proportions of stearic acid in soybean oil were prepared and their microstructures were successfully studied. The micrographs revealed the presence of fiber like structures which are clusters of stearic acid, formed by the self-assembly of gelator molecules as the temperature of the organogel samples decreases. The networked structure helped in the immobilization of the soybean oil. The magneto-organogels also displayed conducting properties even at low concentration in the impedance analysis, which accounts for the fact that it can be used as an electro-responsive gel for controlled drug delivery applications. The release studies of the dye indicated that the organogels may be used as matrix for controlled delivery systems.In short; the organogels developed may be tried as a matrix for controlled drug delivery.

Future scope for magneto-organogel project: This type of organogel will be subjected to thorough impedance study. In general organogel undergoes structural change when high frequency AC signal is passed through it. As this iron oxide based gels have considerable conductance, this materials are expected to carry high frequency AC signal through it and thereby undergo structural change. Such structural change is expected to release any drugs preloaded inside the gel. In other words this magneto organogel has a huge scope of being used as a high frequency AC signal controlled drug delivery agent.

Chapter 2 Gold Nanoparticles

2.1: INTRODUCTION

Nanosciences and Nanotechnology is gaining recent importance in the field of biomedical research. Studies on the impact of the shape and size of the nanoparticles on biological systems have attracted great interests since those help in designing a rational model of nanoparticles for various biomedical applications [21]. Gold nanoparticles possess excellent electronic and optical properties such as surface plasmon resonance (SPR), anti-arthritic activity, anti-bacterial activity, anti-angiogenesis activity, biocompatibility, catalytic activity [22] etc. Surface plasmon resonance property of gold nanoparticles makes them an ideal candidate for bio-imaging and bio-diagnostic purpose. The properties of gold nanoparticles can be tuned by varying the size, shape, surface chemistry or state of aggregation [23]. Gold nanoparticles, also known as gold colloids, can be used for fabrication of smart sensing devices for biomedical applications. Gold nanoparticles have excellent compatibility with antibodies and other biomolecules since their immobilization does not alter the functional activities [24]. Thus it can be specifically used for detection of target analyte. Therefore the synthesis of gold nanoparticles has gained much attention in the past few decades. The major focus is to develop effective synthesis methods to meet the ever increasing demand of gold nanoparticles required for multiple applications. The main objective of this current project work is to synthesize and characterize gold nanoparticles *via* different synthetic routes. This chapter basically focuses on the different techniques applied for synthesizing gold nanoparticles.

Objectives of the study:

The main objectives of this work are as follows:

- To synthesize and characterize gold nanoparticles by citrate reduction approach using hydroquinone and to study the influence of hydroquinone on the nanoparticles.
- To synthesize and characterize gold nanoparticles using green tea extracts.
- To investigate the impact of Cr(II) aqueous solution on gold seeds nanoparticles and to synthesize gold nanoparticles using $CrCl_3$ aqueous solution

2.1.1: Synthesis of Gold nanoparticles using Hydroquinone

Typically the synthesis of gold nanoparticles is carried out using the citrate reduction approach [25]. The citrate reduction method is extensively used because of several advantages such as non-toxic water solvent, inexpensive reducing agent etc. But this approach is capable of producing monodispersed and spherical nanoparticles within a size range of up to 50 nm. The use of stronger reducing agents such as sodium borohydride reduces the size of nanoparticles (2-10 nm) but this technique is generally accompanied by the undesirable secondary nucleation of the smaller nanoparticles. The reducing tendency of the agents plays an important role in influencing the size and properties of the synthesized gold nanoparticles. The ultimate aim is to reduce Au^{III} state of the precursor to Au^0 state of the nanoparticles and the current synthesis focused on the stepwise reduction of Au^{III} to Au^I and then from Au^I to Au^0.In this technique, citrate acts a ligand as well as a reductant [26]. Both citrate and hydroquinone act as reducing agents but play different roles as indicated in the reaction scheme given below. Sodium citrate having weak reducibility at room temperature could reduce Au^{III} to Au^I state while hydroquinone can selectively reduce Au^I to Au^0 state on the surface of gold seeds. The standard reduction potential has been reported to be 1.002 V in the presence of seeds while during the reduction of isolated Au^I to Au^0; the potential was around -1.5 V. Therefore, Hydroquinone selectively reduces Au^I to Au^0 on the surface of seed resulting in the formation of nanoparticles.

Scheme 1: Stepwise reduction of Au(III) to Au(I) by Citrate (Eq. 1) and Au(I) to Au(0) by Hydroquinone (Eq. 2)

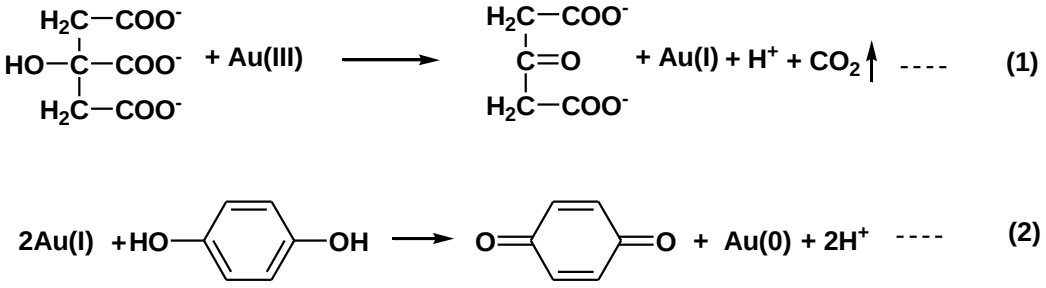

2.1.2: Green Synthesis of Gold nanoparticles using green tea extracts

Tea being the most widely consumed beverages across the globe has well known medicinal properties in today's world. Green tea is produced from the leaves of the plant *Camellia Sinensis* which belongs to Theaceae family [27]. Green tea is mostly regarded as a safe, non-toxic beverage whose consumption does not lead to any kinds of side effects. Instead, Green tea contains several polyphenols such as epicatechin, epigallocatechin etc. which possess significant anti-inflammatory, probiotic, antioxidant, antimicrobial and anti-carcinogenic properties in a wide range of humans and animals. In this technique, the green synthesis of gold nanoparticles (Au NPs) was carried out using a faster, easier, cost-effective and environmental friendly route. Extracts of green tea (*Camellia Sinensis*) was employed for the synthesis of Gold nanoparticles. Presence of polyphenols in green tea extracts facilitates the reduction of Au^{3+} to Au^{0} state thereby contributing to the formation of nanoparticles [28]. Through this work, green synthesis has been attempted to be implemented in the field of Nanosciences since this technique is simple, cost effective, provides long term stability and serves as an alternative to the toxic chemical methods. Therefore, the future works in the areas of nanotechnology must be focused on the utilization of extracts of plant and micro-organisms for the reduction of gold ions. The reaction scheme for the above synthetic route is shown below:

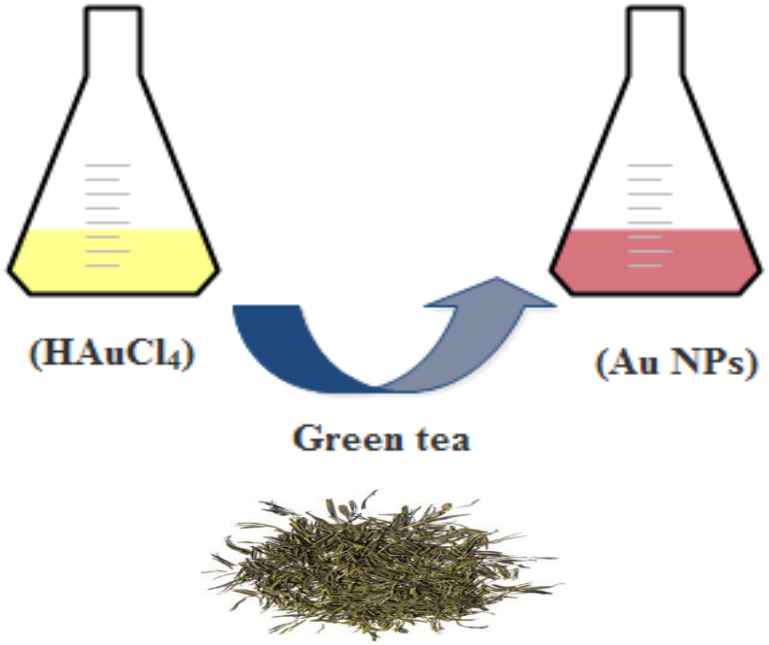

Figure 21: Scheme for the synthesis of gold nanoparticles using green tea extracts

2.1.3: Synthesis of Gold nanoparticles using $CrCl_2$ aqueous solution

$CrCl_2$ dissolves in oxygen free water to give a blue solution of the Cr^{2+} ion. $CrCl_2$ readily dissolves in water to give a bright blue air-sensitive solutions of $[Cr(H_2O)_4]Cl_2$. Cr(II) compounds are oxidized by air to Cr(III). The dihalides of Cr(II) are all readily oxidized in air to the (III) state unless protected by an inert atmosphere such as N_2. $CrCl_2$ is the most important dihalide of chromium and it dissolves in water giving the sky blue coloured $[Cr(H_2O)_6]^{2+}$ ion. d^3 metal ion has a spin allowed d-d electronic transition.

The ion is readily oxidized:

$$\mathbf{Cr^{3+} + e^- \rightarrow Cr^{2+} \quad ; \quad E^0 = -0.41\ V}$$

The current study was focused on the investigation of synthesis of gold nanoparticles using $CrCl_2$ aqueous solution both in the presence and absence of inert atmospheric conditions. The synthesis was carried out in a similar manner as explained in the synthesis of gold nanoparticles using hydroquinone. This experiment was carried out in several parts to investigate the impact of Cr(II) aqueous solution on the synthesis of the nanoparticles. Variation in the amounts of $CrCl_2$ aqueous solution was done along with the addition of Cr(II) aqueous solution to gold seeds nanoparticles [29]. This addition leads to the aggregation of gold nanoparticles marked by distinct colour change and the reaction scheme is illustrated in the diagram given below. This aggregation of nanoparticles has been utilized in many colorimetric assays as a detection mechanism for detecting toxic metal ions such as Hg(II), Cu(II), Cd(II), Cr(III) etc. which acts as potential water pollutants [30].

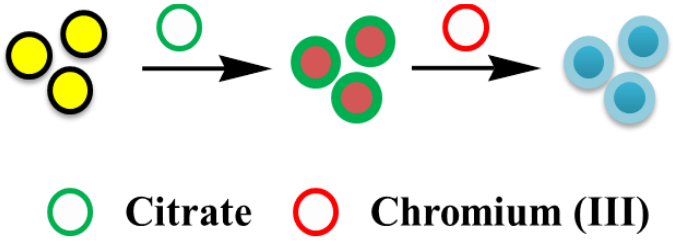

Figure 22: Schematic representation of Au NPs synthesis by $CrCl_3$ reduction method.

2.2: EXPERIMENTAL

2.2.1: Synthesis of gold nanoparticles using hydroquinone

Materials: gold (III) chloride ($HAuCl_4.3H_2O$) (FINAR Reagents), sodium citrate ($C_6H_5Na_3O_7.2H_2O$) (AR Grade, Merck), hydroquinone ($C_6H_6O_2$) (SRL Pvt. Ltd.) were obtained commercially and used as received. De-ionized water was obtained from Sigma Aldrich.

(a) Synthesis of gold seeds: For the preparation of gold seeds, 100 mM $HAuCl_4$ aqueous solution was foremost prepared by dissolving $HAuCl_4$ (25.0 mg) in de-ionized water (635 µL). A 100 µL of the above solution was put into a flask with 40 ml of de-ionized water under vigorous stirring (500 rpm) and heated to boil (100-120^o C). As soon as the solution started boiling, 1200 µL of 1 w/v % of sodium citrate aqueous solution (10mg/ml) was added to it and it was kept at boiling until the solution turned wine red coloured. The solution was allowed to cool down to room temperature under stirring to obtain the gold seeds.

(b) Synthesis of gold nanoparticles: The 30 mM hydroquinone solution was prepared by dissolving 33 mg of solid hydroquinone in 10 ml de-ionized water. For the synthesis of nanoparticles, aqueous solution of 100 mM $HAuCl_4$ (11.2 µL, 0.5 µmol) was added to de-ionized water (9.6 ml) under vigorous stirring (500 rpm). Subsequently, a mixture of gold seeds (50 µL), 1% sodium citrate (22 µL) and 30mM hydroquinone (1000 µL) was added to it. The solution was kept under stirring at room temperature for 30 minutes to obtain the nanoparticles. The above steps were repeated by altering the amount of 30 mM hydroquinone aqueous solution from 200 µL, 500 µL to 2000 µL. The entire procedure was again repeated by altering the amount of 100 mM $HAuCl_4$ aqueous solution (33.6 µL, 1.5 µmol) with the same amounts of gold seeds and sodium citrate and altering the amounts of hydroquinone from 200, 500, 1000 to 2000 µL. The growth duration of all samples was 30 minutes.

2.2.2: Synthesis of gold nanoparticles using green tea extracts

Materials: gold (III) chloride ($HAuCl_4.3H_2O$) (FINAR Reagents), sodium citrate ($C_6H_5Na_3O_7.2H_2O$) (AR Grade, Merck), green tea (Organic India Pvt. Ltd.) were obtained commercially and used as received. De-ionized water was obtained from Sigma Aldrich.

(a) Synthesis of green tea extracts: For the preparation of green tea, Green tea extracts (500 mg) was added to de-ionized water (50 ml) in flask with vigorous stirring (500 rpm) and heated to boil for about 2 minutes. The reddish brown colour tea extract was then filtered to remove the solid undissolved residues of tea leaves. This reddish brown coloured filtrate was then collected in centrifuge tubes and was used for preparation of gold nanoparticles by reduction of gold chloride solution.

(b) Synthesis of gold nanoparticles: For the synthesis of nanoparticles, 100 mM $HAuCl_4$ aqueous solution was foremost prepared by dissolving $HAuCl_4$ (25.0 mg) in de-ionized water (635 µL). A 33.6 µL of the above solution was put into a flask with 40 ml of de-ionized water under vigorous stirring (500 rpm) and heated to boil (100-120^o C). As soon as the solution started boiling, 1200 µL of 1 w/v % of sodium citrate aqueous solution (10mg/ml) and 2000 µL of green tea was added to it and it was kept at boiling until the solution turned wine red coloured. The solution was allowed to cool down to room temperature under stirring to obtain the gold seeds.

Another procedure involved the addition of aqueous solution of 100 mM $HAuCl_4$ (33.6 µL, 1.5 µmol) to de-ionized water (9.6 ml) under vigorous stirring (500 rpm). Subsequently, gold seeds (50 µL), 1% sodium citrate (22 µL) and green tea (1000 µL) was added to it one by one. The solution was kept under stirring at room temperature for 30 minutes to obtain the nanoparticles. The above steps were repeated by altering the amount of green tea extract solution from 200 µL, 500 µL to 2000 µL. The growth duration of all samples was 30 minutes.

2.2.3: Synthesis of gold nanoparticles using $CrCl_2$ aqueous solution

Materials: gold (III) chloride ($HAuCl_4.3H_2O$) (AR Grade, FINAR Reagents), sodium citrate ($C_6H_5Na_3O_7.2H_2O$) (AR Grade, Merck), chromium (II) chloride ($CrCl_2$) (Sigma-Aldrich) were obtained commercially and used as received. De-ionized water was obtained from Sigma-Aldrich.

(a) Synthesis of gold nanoparticles: 100 mM $HAuCl_4$ aqueous solution was foremost prepared by dissolving $HAuCl_4$ (25.0 mg) in de-ionized water (635 µL). A 100 µL of the above solution was put into a flask with 40 ml of de-ionized water under vigorous stirring (500 rpm) at room temperature. 1200 µL of $CrCl_2$ aqueous solution (30 mM) was added to it and it was kept at stirring for 10 minutes. The entire procedure was repeated under inert atmospheric conditions by

connecting a N_2 gas filled balloon to the flask. The solution turned wine red in colour immediately after the addition of $CrCl_2$ aqueous solution to it under inert atmospheric conditions.

Another set of experiment involved the addition of aqueous $HAuCl_4$ solution (25 μL, 100 mM) into de-ionized water (9.6 ml) under vigorous stirring at room temperature. Subsequently, gold seeds (50 μL), 1% sodium citrate (22 μL) and $CrCl_2$(1000 μL, 30 mM) aqueous solution was added one by one. The solution was kept under stirring at room temperature for 15 minutes. The experiment related to this part was conducted both under the presence and absence of inert atmosphere. In the presence of inert atmosphere, the solution turned wine red colour within few minutes after addition of $CrCl_2$ aqueous solution (30 mM). In the absence of inert atmosphere, the solution turned dark blue/ grey almost similar to colour of the $CrCl_2$ aqueous solution.

(b) Synthesis of aggregated gold nanoparticles: A solution of Au seeds nanoparticles (28 ml) was taken in a flask under vigorous stirring at room temperature and $CrCl_2$ aqueous solution (20 ml, 30 mM) was added to it and the solution was stirred for 15 minutes. This part was carried out both in the presence and absence of inert atmosphere. The inert atmospheric conditions had the final solution turning deep blue coloured as observed in the case of addition of hydroquinone to obtain gold nanoparticles. Mixing ratio of gold seeds and $CrCl_2$ aqueous solution was about 1.4:1. The entire procedure was again carried out with 1 mM $CrCl_2$ aqueous solution

2.3: RESULTS AND DISCUSSION

Characterization analysis: Scanning electron microscopy (SEM) was conducted in FEI-FESEM (Nova nano SEM) operated at 5 kV. UV-visible absorbance was measured using Shimadzu, UV-2450 Spectrophotometer. XRD Analysis was done using X-ray diffractometer Rigaku X-ray diffractometer with Cu K_α source. DLS study and Zeta potential analysis was carried out using Malvern Zeta Sizer.

2.3.1: UV-visible spectroscopy analysis

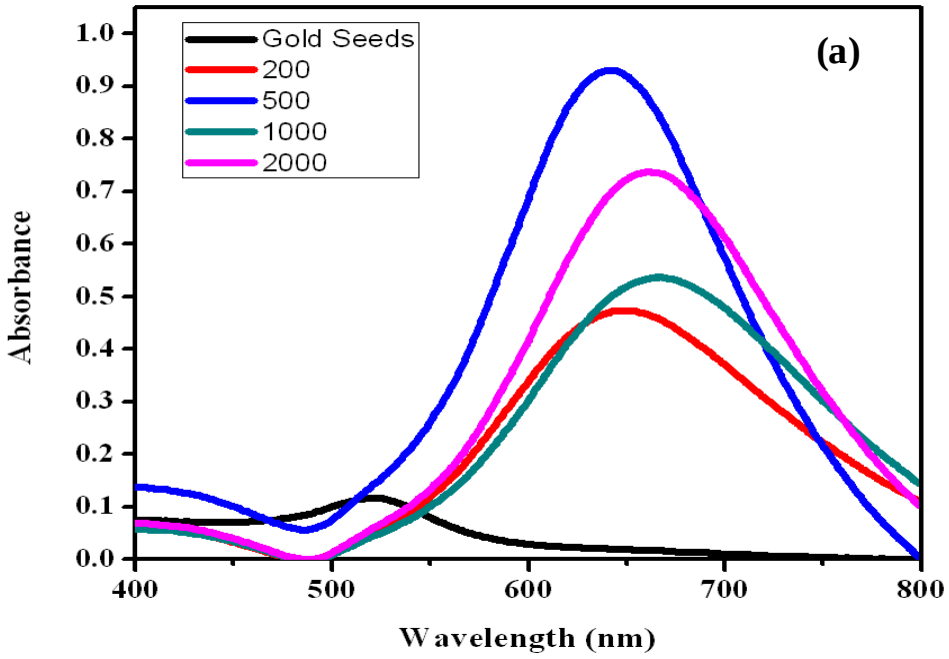

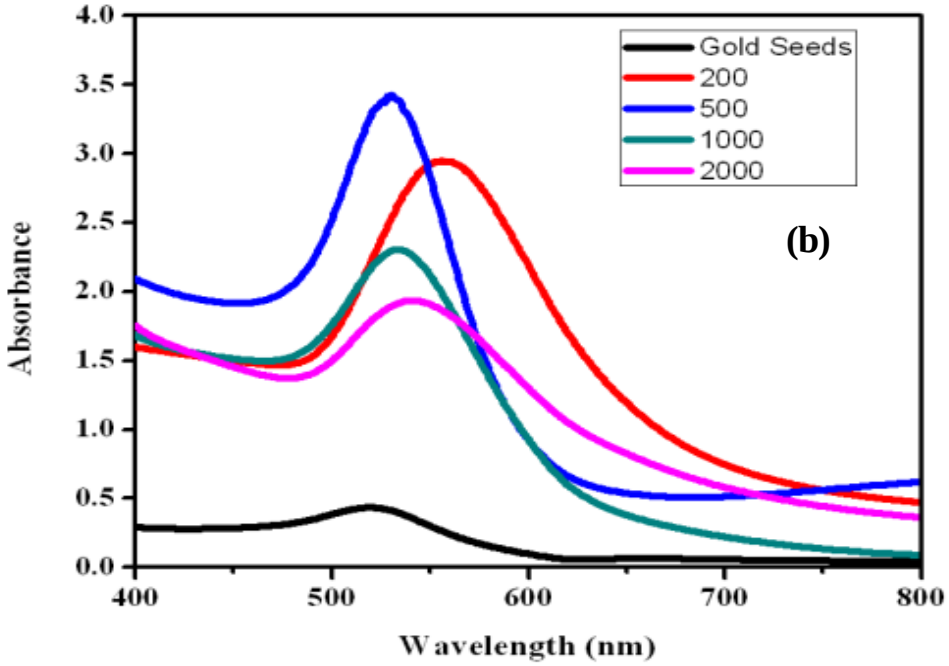

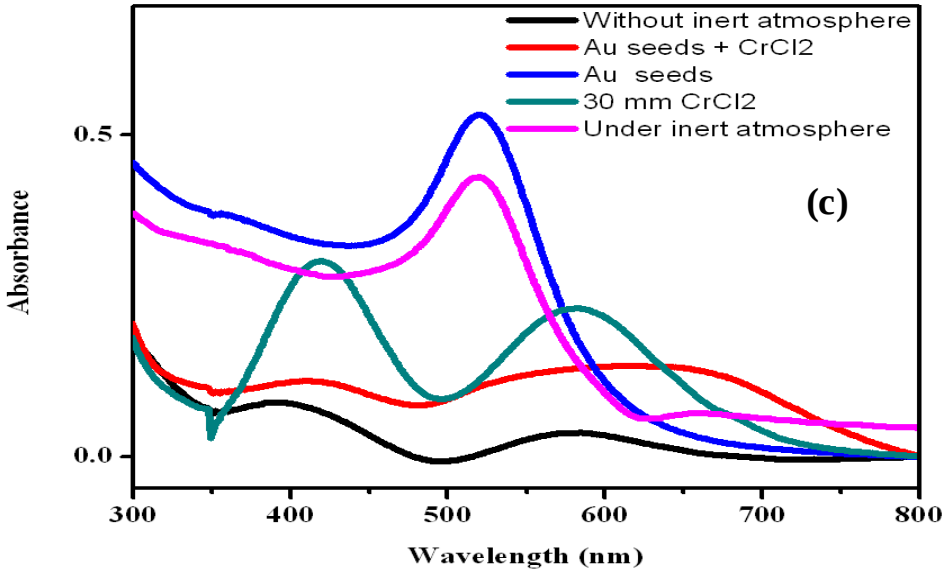

Figure 23: UV-visible absorption spectra of (a) HQ mediated synthesized Au NPs; (b) Green Tea mediated synthesized Au NPs; (c) $CrCl_2$ mediated synthesized Au NPs

The absorption bands originated from the surface optical property of gold exhibited only at nano dimension, known as surface plasmon resonance (SPR). With the increase in the concentration of hydroquinone added, the plasmon absorption of gold NPs shifted from 521 to 652 nm (Fig. 23(a)), typical for an increase of NP diameters. The increased concentration of hydroquinone clearly led to the aggregation of gold nanoparticles marked by shift in the SPR peaks. The Ultraviolet-Visible spectroscopy (400 -800 nm) range showed absorption bands with sharp peaks (535 - 565 nm) for green tea mediated synthesis (Fig. 23 (b)).Appearance of SPR bands confirmed the formation of Au NPs from green tea extracts. Figure 23(c) clearly indicates maximum wavelength of the synthesized sample under inert atmospheric condition as 522 nm and the spectrum is very similar to spectrum of gold seeds which shows maximum wavelength as 521 nm. In the same figure, spectrum of the sample prepared without inert atmospheric condition is quite similar to the spectrum of $CrCl_2$ aqueous solution (30 mM) indicating that the resulting solution is essentially Cr(II) solution or a citrate complex of Cr(II). When gold seeds NPs interacted with the Cr(II) solutions, there was an immediate intense colour change from wine red to blue accompanied with a red shift in the SPR peak from 526 nm to 690 nm, indicating the

aggregation of gold NPs. Therefore under inert atmospheric condition, the surface Plasmon resonance peak is obtained at 522 nm which matches well for gold nanoparticles.

2.3.2: XRD Analysis

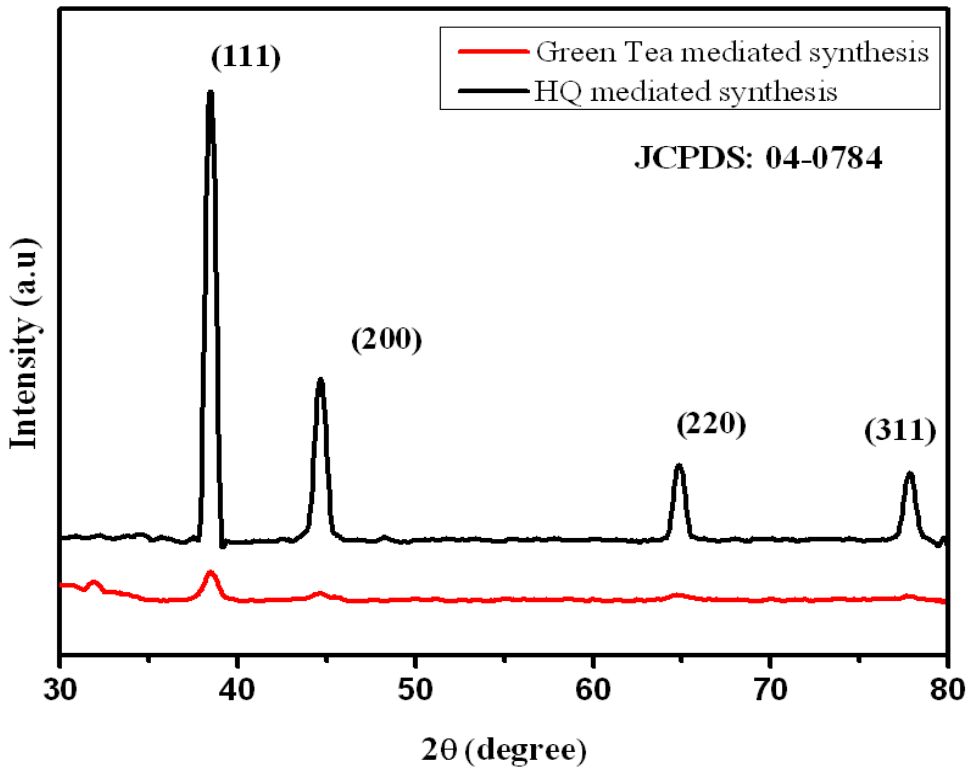

Figure 24: XRD pattern of the synthesized gold nanoparticles

XRD analysis of the Au NPs exhibited Bragg's reflections, which was indexed on the basis of the face centred cubic (FCC) gold structure. The diffraction peaks (111), (200) and (220) corresponding to 38.1 ˚, 44.5 ˚ and 64.8 ˚ 2θ angles, respectively, confirmed that the synthesized Au NPs were of crystalline nature. A strong diffraction peak located at 38.15 ˚ was ascribed to the (111) facets of face-centred cubic metal gold structures, while diffraction peaks of other facets were much weaker. The diffraction peaks of green tea mediated synthesized Au NPs matched well with the standard diffraction peaks (JCPDS Card No: 04-0784) but were observed to be of very low intensity.

2.3.3: FESEM Analysis

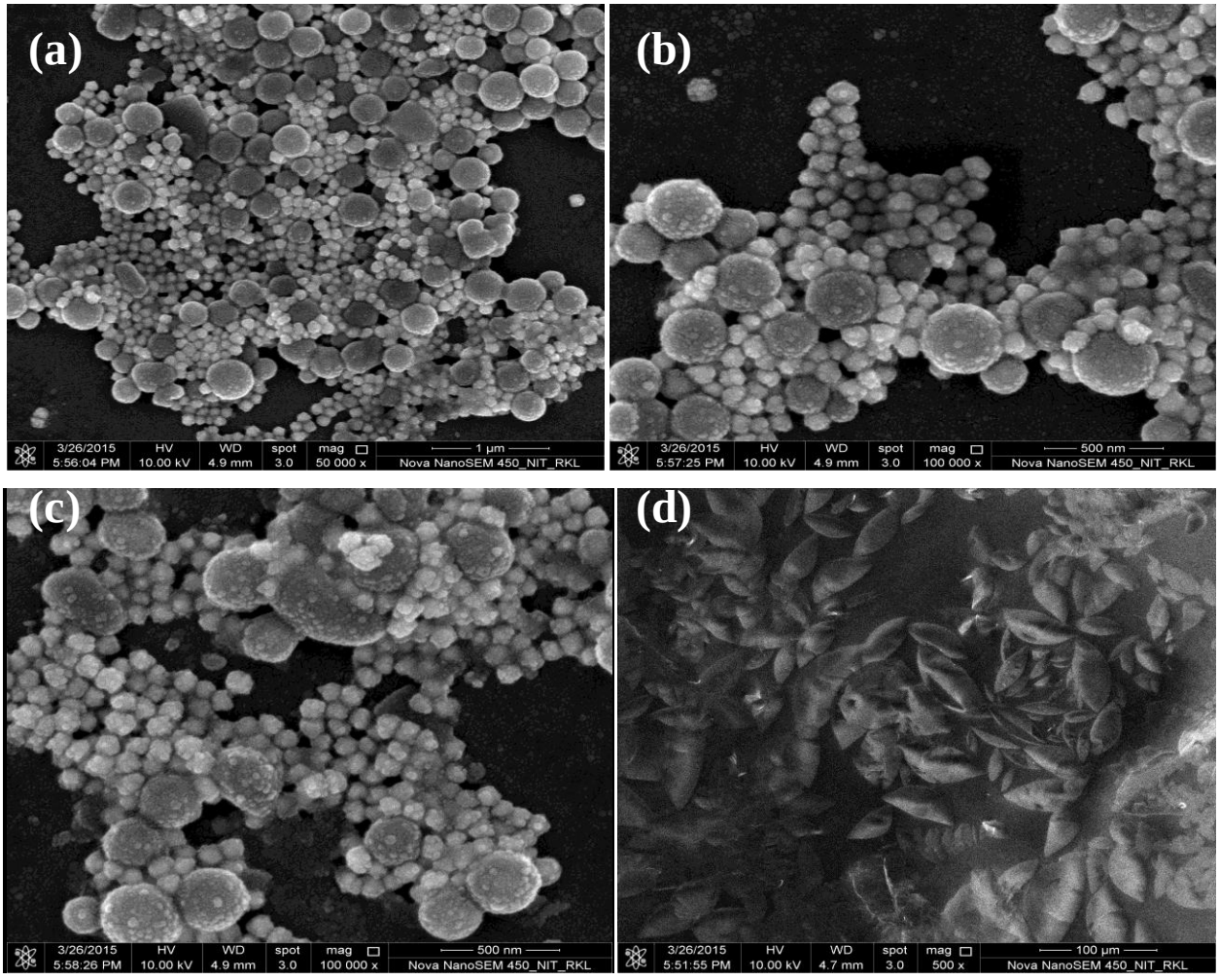

Figure 25: FESEM images of gold nanoparticles obtained from HQ (a), (b), (c) and obtained from green tea (d)

The FESEM images showed relatively spherical shaped nanoparticles formed with average diameter in the range of 100 ± 5 nm. The spot profile EDAX of Au NPs showed a strong signal for gold, confirming the successful formation of Au NPs. Moreover, the FESEM images show that most of the gold nano- spheres are round or spherical in shape. The FESEM images of green tea mediated synthesized samples are mostly tubular shaped possibly due to the aggregation of the nanoparticles (fig. 25 (d)).

2.3.4: DLS Study

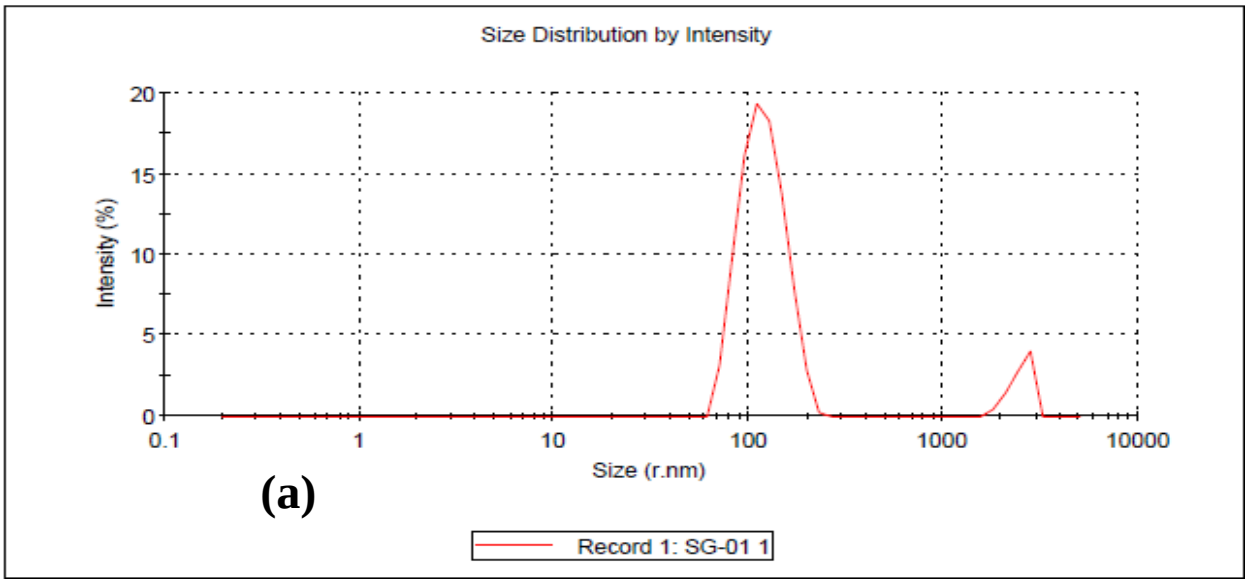

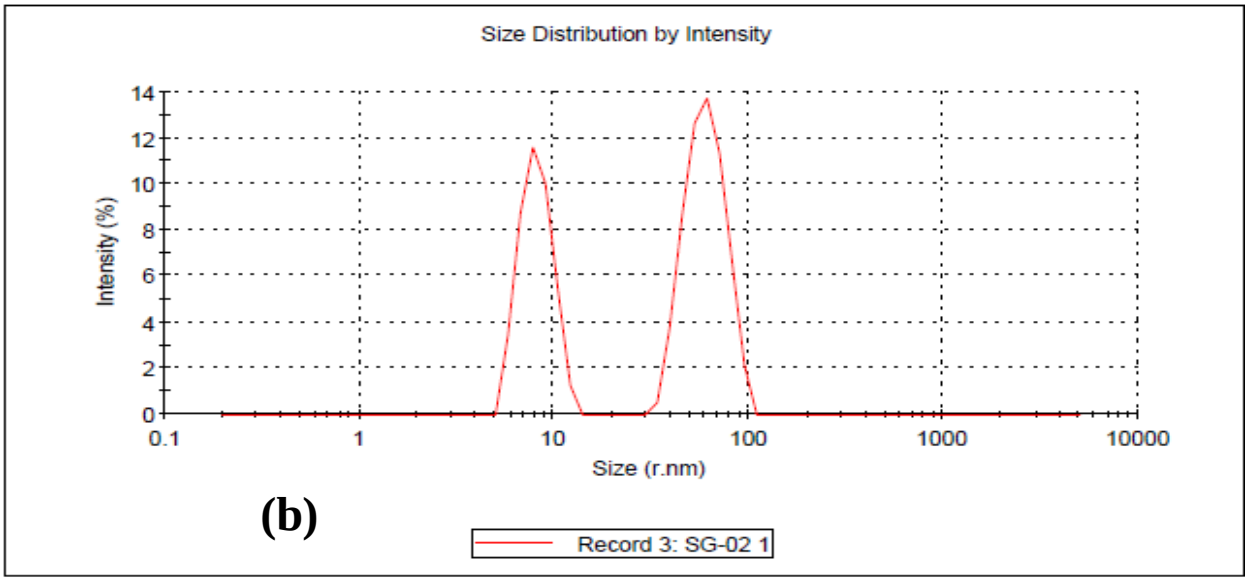

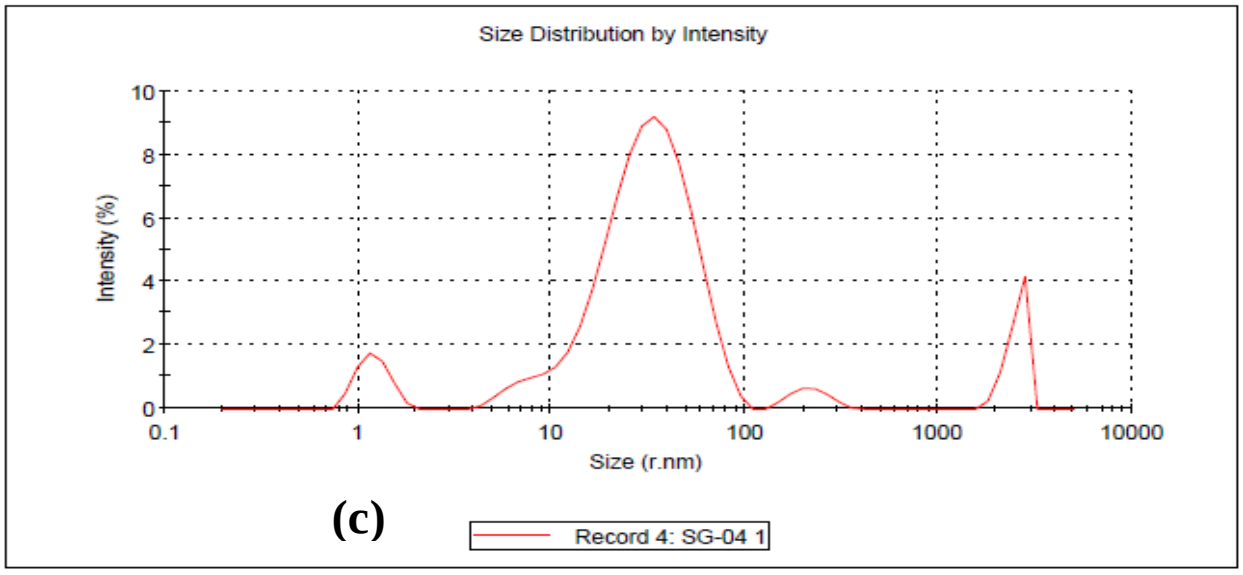

Figure 26: Particle size distribution curve of (a) Au NPs synthesized from 200 µL HQ; (b) Au seeds NPs; (c) Au NPs synthesized from 2000 µL Green Tea extracts

Dynamic light scattering (DLS) analysis determined the average particles size distribution profile of synthesized gold nanoparticles. In our result, the size of Au NPs is in the range 60-140 nm and average size is 120 nm for HQ mediated synthesis (Fig.26(a)) while the size range is 5-100 nm and average size is 32 nm (Fig.26(c)). In addition, some of the large sized particles appeared in DLS result, which is due to the agglomeration Au NPs in the solution.

2.3.5: Zeta Potential Distribution:

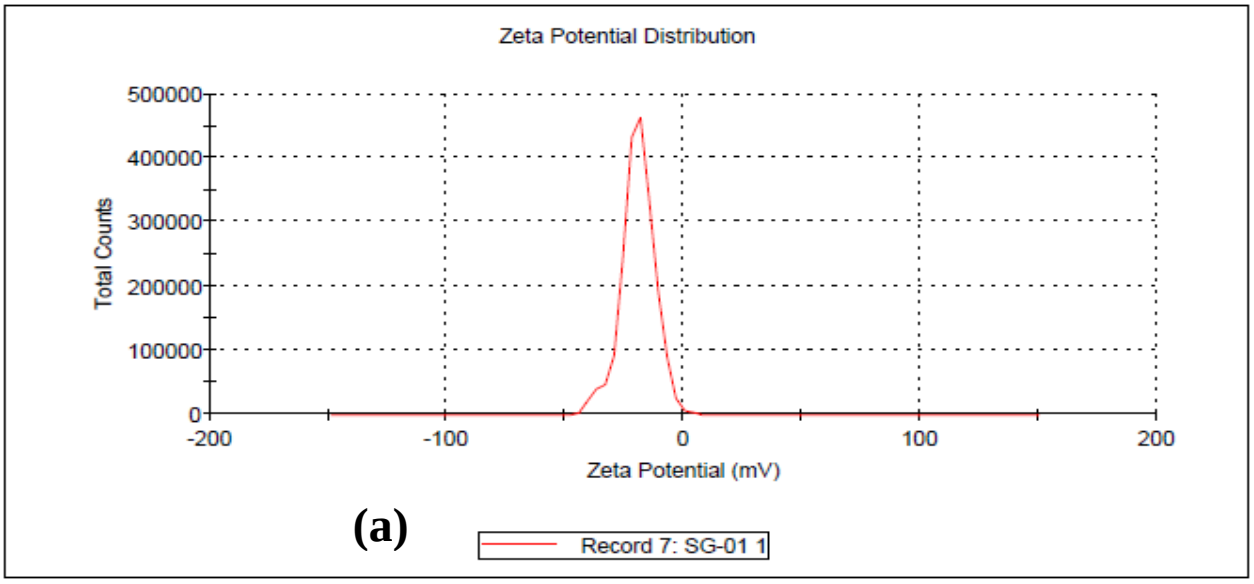

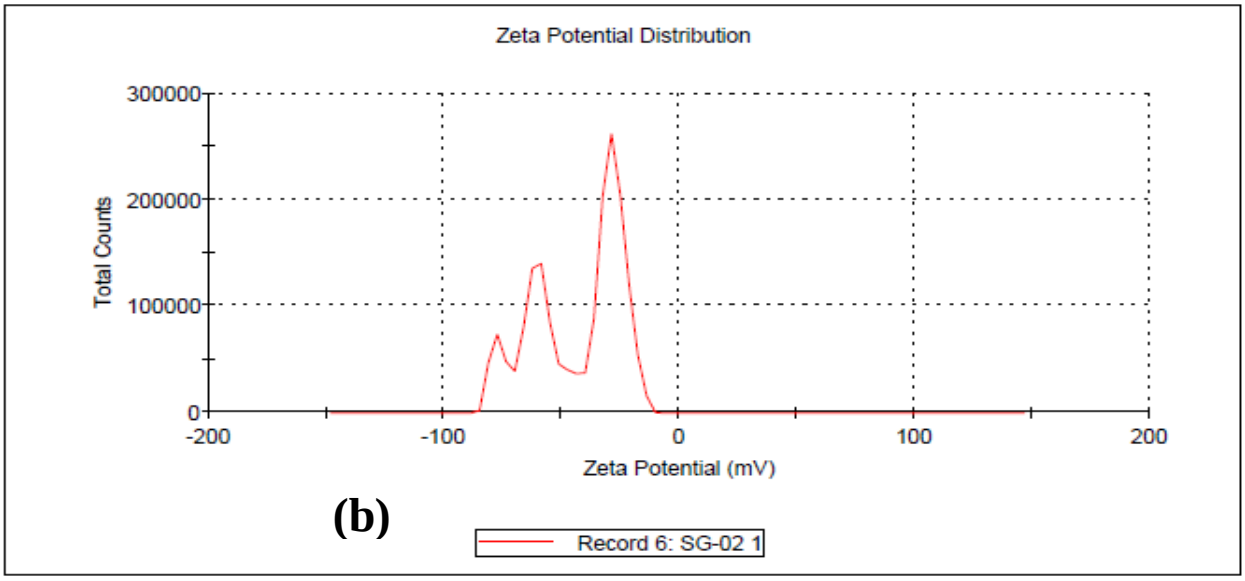

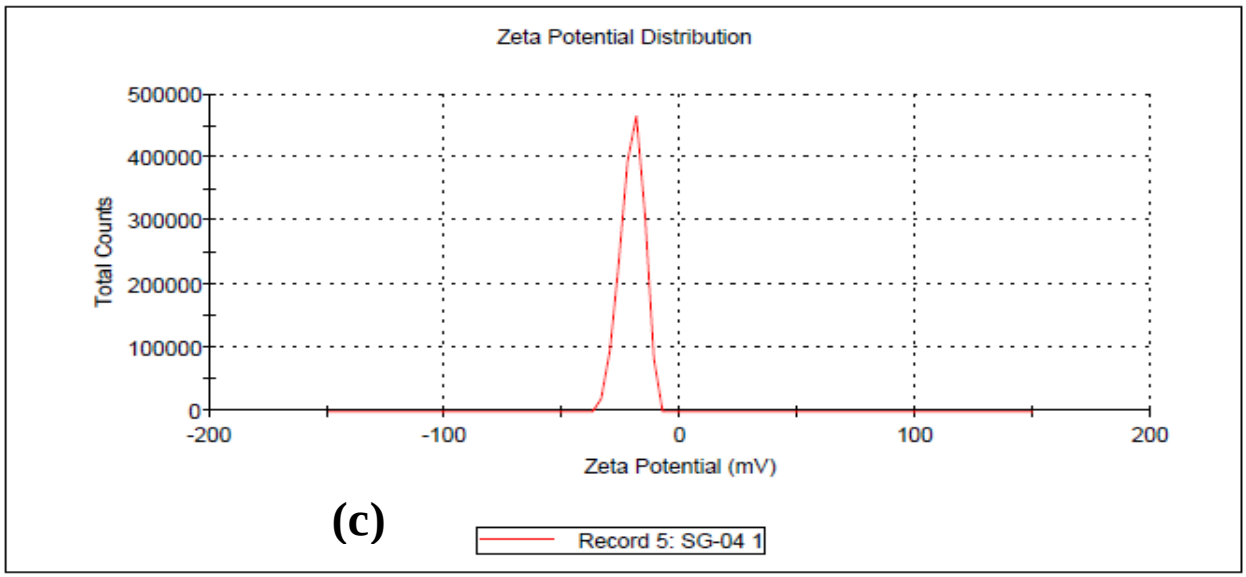

Fig.27: Zeta potential distribution of (a) Au NPs synthesized from 200 µL HQ; (b) Au seeds NPs; (c) Au NPs synthesized from 2000 µL Green Tea extracts

Zeta potential (ZP) analysis provided clear information on the surface charge as well as stability of the synthesized nanoparticles. In our study, ZP value of the synthesized Au NPs is -19.2 mV for HQ mediated synthesis (Fig.27 (a)) while for Green Tea mediated synthesis, the ZP value was observed to be -20.4 mV. Au seeds NPs exhibited a ZP value of -43.3 mV. The negative charge on nanoparticles due to citrate ions is an important indicator for particle size. In present study, zeta potential of gold nanoparticles was highly negative.

2.4: CONCLUSIONS

The present work was carried out to investigate the synthesis and characterization of gold nanoparticles. The uniform gold nanoparticles with small size can be synthesized from the tetrachloroauric acid precursor at high concentration by the citrate reduction method. In summary, we demonstrated a seed-mediated growth of gold NPs by varying the concentration of hydroquinone making it possible to tune the diameters of as-prepared NPs from 50 to 150 nm.We report here the application of a plant mediated green synthesis approach for the synthesis of gold nanoparticles from $HAuCl_4 \cdot 3H_2O$ by using green tea extracts (*Camellia Sinensis)* as reducing, stabilizing or capping agent. The advantages of this synthesis are it is a simple, low cost, stable for long time, eco-friendly, green chemistry approach, alternative to other biological, physical and chemical methods. In chromium chloride mediated synthesis, Cr (III) can serve as effective cross linking agent between the pairs of citrate-coated Au NPs, leading to the aggregation of the Au NPs. The aggregation of the nanoparticles may drastically alter the surface plasmon oscillation in metallic nanoparticles since the individual particles can be electronically coupled to each other [interparticle plasmonic coupling]. As a result, their plasmon resonance is red-shifted, causing the colour in transmission to become blue from wine red. The characterization of Au NPs was done with UV-Vis study which exhibited the typical surface plasmon resonance property of the colloidal solution. The as prepared Au NPs solution, wine red in colour exhibited a strong surface plasmon resonance peak at 521 nm as also observed in prior studies [32].XRD patterns and FESEM images confirmed the formation of spherical gold nanoparticles while the size distribution analysis was carried out from DLS and Zeta Potential studies.

Future scope for gold nanoparticle project: Based on the studies conducted here, several pathways of making gold nanoparticles of average size larger than 20 nm can be utilized. Citrate reduction method yields gold nanoparticle seeds having diameter around 20 nm. On further reduction of Au(III) to Au(0), the seeds can be grown in size. In future, using either hydroquinone reduction method or green tea reduction method gold nanoparticles of different shapes and sizes can be synthesized.

REFERENCES

[1] Indira, T.K.; Lakshmi, P.K. *International Journal of Pharmaceutical Sciences and Nanotechnology*, **2010**, 3, 1035-1042

[2] Laurent, S.; Forge, D; Port, M.; Roch, A.; Robic, C.; Elst, L.V.; Muller, R.N. *Chem.Rev.*, **2008**, 108, 2064-2110

[3] Kim, D.K.; Zhang, Y.; Voit, W.; Rao, K.V.; Muhammed, M. *Journal of Magnetism and Magnetic Materials*, **2001**, 225, 30-36

[4] Petcharoen, K.; Sirivat, A. *Material Science and Engineering B*, **2012**, 177, 421-427

[5] Ou, P.; Xu, G.; Xu, C.; Zhang, Y.; Hou, X.; Han, G. *Materials Science –Poland*, **2010**, 28, 817-822

[6] Giri, S.; Li, Dawei; Chan. C. W. *Chem. Commun.*, **2011**, 47, 4195-4197

[7] Shaker, S.; Zafarian, S.; Chakra C.H.S.; Rao, K.V. *Innovative Research in Science, Engineering and Technology*, **2013**, 2, 2969-2973

[8] Lei, P.; Boeis, A.M.; Calder, S.; Girshick, S.L. *Plasma Chem Plasma Process*, **2012**, 32,519-531

[9] Sundar, S.; Piraman, S. *Indian Journal of Applied Research*, **2013**, 3, 123-126

[10] Kandpal, N.D.; Sah, N.; Loshali, R.; Joshi, R.; Prasad, J. *Journal of Scientific and Industrial Research*, **2014**, 73, 87-90

[11] Ou, P.; Xu, G.; Xu, C.; Zhang, Y.; Hou, X.; Han, G. *Materials Science –Poland*, **2010**, 28, 817-822

[12] Ge, S.; Shi, X.; Orr, B.G. *J. Phys. Chem. C. Nanomater Interfaces*, **2009**, 113, 13593-13599

[13] Chin, S.F.; Pang, S.C.; Tan, C.H. *J.Mater.Environ.Sci*, **2011**, 2, 299-302

[14] Gui, M.; Smuleac, V.; Ormsbee, L.E.; Sedlak, D.L.; Bhattacharyya, D. *J.Nanopart Res*, **2012**, 861, 1-16

[15] Laouini, A.; Jaafar-Maalej, C.; Limayem-Blouza, I.; Sfar, S.; Charcosset, C.; Fessi, H. *Journal of Colloid Science and Biotechnology*, **2012**, 1, 147-168

[16] Gonzales, M.; Krishnan K.M. *Journal of Magnetism and Magnetic Materials*, **2005**, 293, 265-270

[17] Vintiloiu, A.; Leroux, J.C. *Journal of Controlled Release*, **2008**, 125, 179-192

[18] Murdan, S.; Gregoriadis, G.; Florence, A.T. *Journal of pharmaceutical sciences*, **1999**, 88, 608-614

[19] Teixeira, A.C.T.; et al. *Chemistry and Physics of Lipids*, **2010**, 163, 655-666

[20] Mallia, V.A.; Terech, P.; Weiss, R.G. *The Journal of Physical Chemistry B*, **2011**,115, 12401-12414

[21] Jain, P.K.; Lee, K.S.; El-Sayed, I.H.; El-Sayed, M.A. *J. Phys. Chem. B*, **2006**, 110, 7238-7248

[22] Boisselier, E.; Astruc, D. *Chem. Soc. Rev.*, **2009**, 38, 1759-1782

[23] Daniel, M.C.; Astruc, D. *Chem. Rev.*, **2004**, 104, 293-346

[24] Li, D.X.; Li, C.F.; Wang, A.H.; He, Q.; Li, J.B. *J. Mater. Chem.*, **2010**, 20, 7782-7790

[25] Ji, X.H.; Song, X.N.; Li, J.; Bai, Y.B.; Yang, W.S.; Peng, X.G. *J. Am. Chem. Soc.*, **2007**, 129, 13939-13948

[26] Li, Jing; Wu, J.; Zhang, X.; Liu,Y.; Zhou, D.; Sun, H.; Zhang H.; Yang B. *J. Phys. Chem. C*, **2011**, 115, 3630–3637

[27] Ahmad, N.; Feyes, D.K.; Nieminen, A.L.; et al. *J Natl Cancer Inst.*, **1997**, 89, 1881-1886

[28] Boruah, S. K.; Boruah, P. K.; Sarma, P.; Medhi, C.; Medhi, O. K. *Adv. Mat. Letters*, **2012**, 3, 481-486

[29] Mukherjee, A.; Chandrasekaran, N.; Rajeshwari, A.; Elavarasi, M. *Analytical Methods*, **2013**, 5, 6211-6218

[30] Ding, N.; Cao, Q.; Zhao, H.; Yang, Y.; Zeng, L.; He, Y.; Xiang, K.; Wang, G. *Sensors*, **2010**, 10, 11144-11155.